

Received 12 August 2022, accepted 31 August 2022, date of publication 5 September 2022, date of current version 16 September 2022.

Digital Object Identifier 10.1109/ACCESS.2022.3204618

## RESEARCH ARTICLE

# An Incentivized and Optimized Dynamic Mechanism for Demand Response for Managing Voltage in Distribution Networks

MD MOKTADIR RAHMAN<sup>1</sup>, ALI AREFI<sup>2</sup>, (Senior Member, IEEE), G. M. SHAFIULLAH<sup>1b2</sup>, SUJEEWA HETTIWATTE<sup>3</sup>, ALI AZIZVAHED<sup>4</sup>, S. M. MUYEEN<sup>1b5</sup>, (Senior Member, IEEE), AND MD. RABIUL ISLAM<sup>1b6</sup>, (Senior Member, IEEE)

<sup>1</sup>Essential Energy, Port Macquarie, NSW 2444, Australia

<sup>2</sup>Discipline of Engineering and Energy, Murdoch University, Perth, WA 6150, Australia

<sup>3</sup>Faculty of Engineering, Electrical & Electronic Engineering, Sri Lanka Institute of Information Technology, Malabe 10115, Sri Lanka

<sup>4</sup>School of Electrical and Data Engineering, University of Technology Sydney, Broadway, NSW 2007, Australia

<sup>5</sup>Department of Electrical Engineering, Qatar University, Doha 2713, Qatar

<sup>6</sup>School of Electrical, Computer and Telecommunications Engineering, University of Wollongong, Wollongong, NSW 2522, Australia

Corresponding author: S. M. Mueeen (sm.mueeen@qu.edu.qa)

The publication of this article was funded by Qatar National Library.

**ABSTRACT** The voltage regulation in distribution networks is one of the major obstacles when increasing the penetration of distributed generators (DGs) such as solar photovoltaics (PV), especially during cloud transients, causing potential stress on network voltage regulations. Residential demand response (DR) is one of the cost-effective solutions for voltage management in distribution networks. However, the main barriers of DR implementation are the complexities of controlling a large number and different types of residential loads, satisfying customers' preferences and providing them fair incentives while identifying the optimum DR implementation locations and sizing as well as cooperating with the existing network equipment for the effective voltage management in the networks. A holistic and practical approach of DR implementation is missing in the literature. This study proposes a dynamic fair incentive mechanism using a multi-scheme load control algorithm for a large number of DR participants coordinating with the existing network equipment for managing voltage at medium voltage (MV) networks. The multi-scheme load control is comprised of short-interval (10-minute) and long-interval (2-hour) DR schemes. The dynamic incentive rates are optimized based on the energy contribution of DR participating consumers, their influence on the network voltage and total power loss improvement. The proposed method minimizes the DR implementation cost and size, fairly incentivizes the consumers participating in the DR and priorities their consumption preferences while reduces the network power losses and DGs' reactive power contributions to effectively manage the voltage in the MV networks. An improved hybrid particle swarm optimization algorithm (IHPSO) is proposed for the load controller to provide fast convergence and robust optimization results. The proposed approach is comprehensively tested using the IEEE 33-bus and IEEE 69-bus networks with several scenarios considering a large number of DR participants coordinated with the DGs and on-load tap changer (OLTC) in the networks.

**INDEX TERMS** Cloud transients, consumer comfort, distribution networks, dynamic fair incentive, load control, voltage management, distributed generation, solar photovoltaics.

## I. INTRODUCTION

Over the recent years, the use of renewable energy sources (RESs) in the form of distributed generators (DGs) have

The associate editor coordinating the review of this manuscript and approving it for publication was Lei Chen <sup>1b</sup>.

increased considerably [1]. The conventional distribution systems have not been designed with the consideration of bidirectional power flows from the RESs, which create major challenges for distribution system operators to maintain the system reliability and power quality within the standard limits. Cloud-induced transients over the solar photovoltaic

(PV)-based DGs are considered as one of the potential barriers for further increase of the PV penetration in the distribution networks [2]. If clouds sweep over the solar catchment area within a short time (in the scale of minutes), the PV power contribution drops quickly which

may cause voltage drop at some buses, especially in remote ones [3]. Such transients can cause voltage deviations beyond the standard range [1] and excessive operation of the network equipment for the voltage regulation [2]. Some conventional approaches for managing voltage in the medium voltage (MV) distribution systems are the on-load tap changer (OLTC) mechanism of the transformer, step voltage regulators, and static volt-ampere reactive (VAR) compensators [1], [4]. However, these methods cannot guarantee that the voltage profile will be within the acceptable bounds throughout all connected feeders to an affected transformer [3]. Also, the lifetime of such operating equipment dramatically reduces because of the increased number of actions needed to handle the voltage deviations due to sudden changes in PV generations [4]. In addition, researchers in [5] have introduced a two-level voltage control in the distribution level including the upper-level optimal reactive power dispatch and lower-level real-time control. In the lower level, the rooftop PVs form an aggregator, then the aggregators are governed by the introduced droop controllers in the MV networks. In the upper level, according to the network condition, the PV will be dispatched to minimize the active power loss in the network. Similarly, the study in [6] has introduced a new approach for voltage regulation in the distribution level using a three-level coordinated control method for the PV inverters. The introduced approach includes a ramp-rate control, and a droop control in the local level of voltage regulation, and the third level control based on dynamic average consensus in the case where the first two levels are not enough to retain the voltage level in the predefined boundaries. However, from the financial perspective, the motivation for the participation of rooftop PVs has not been investigated in these works.

Also, it is important to mention that in most of the distribution networks, there is no incentive for the reactive power support provided by inverters. This reactive contribution is now included in the corresponding standards especially for small-scale inverter-interfaced PV systems, so the owners would not get paid for this contribution. Therefore, the owners of the private owned DGs intend to allocate most of their capacity of generation to generate active power to maximize their profit. However, in the framework here, the reactive power is provided by the large DGs through the optimization process. In other words, the local generation of the reactive power has been done by DGs with a large capacity, which they have enough capacity for generating both active and reactive power. Also, these large DGs are incentivized for their reactive power contributions. Another important fact is that due to the high resistance/reactance ( $R/X$ ) ratio in the distribution networks, the impact of the active and reactive powers changes on the voltage variation are not the same, and in some cases, the effect of the active power change in

voltage variation is higher than the reactive power. Therefore, unlike the transmission networks, the voltage magnitude in the distribution networks can be controlled by the active power from the consumers through demand response (DR) programs effectively.

Therefore, one of the promising means of utilizing the existing infrastructure for managing network voltage is the optimal control of end-users' loads through DR programs [7], [8], [9] incorporated with home energy management systems (HEMSs) [10], [11]. Utilities can communicate with the consumers' HEMSs, which can switch ON and OFF the DR participated appliances almost instantaneously and enable them to react fast to maintain the network voltage effectively [12]. It can postpone the investments on the generation resources and network upgrades [13]. HEMS helps utility for DR implementation by providing information such as household appliances' real-time energy consumption status and consumption preferences set by consumers and by receiving load control signals from the utility to control the appliances. HEMSs are developed considerably over the past years, and the smart grid technologies like smart metering and appliances for load control via HEMS are becoming more attractive for the modern distribution networks [11], [12]. One of the main challenges in the implementation of DR is how to fairly incentivize participants for encouraging them to contribute on a DR program. The incentives to the participating consumers in a DR program should not be fixed or equal across all conditions in a network during an event of voltage or thermal limits violations, namely defined as the DR event in this paper. An incentive scheme should be fair based on the DR participant consumers contribution in each DR event and their locations within the network. A study in [14] propose a fair incentive mechanism for the customers to improve the power quality problems in the network. In the following, the literature of the subject will be investigated in more detail.

The growing penetration of electric vehicles into the distribution network may create huge challenges, which require proper optimized operation for the distribution network [15]. A study in [16] developed a strategy for peak shaving in the distribution network via electric vehicle aggregators which in turn leads to cost reduction and oversaturation of the distribution transformers. Authors in [17], [18], and [19] propose an optimal planning for renewable generators implementation and electric vehicle operations to minimize the voltage deviations and power flow from the main grid as well as minimize the power loss in the microgrids. Likewise, in [20] and [21], demand response program in the presence of an energy management scheme was provided to optimally schedule the electric vehicles as well as adjust the household appliances. The study in [22] developed a reward-based load control algorithm to shave network peaks, where consumers' and utility's profits are considered. It shows that the proposed reward-penalty can move forward the organized operational characteristics and relieve the top bounce back without forcing more costs on consumers. However, only a limited

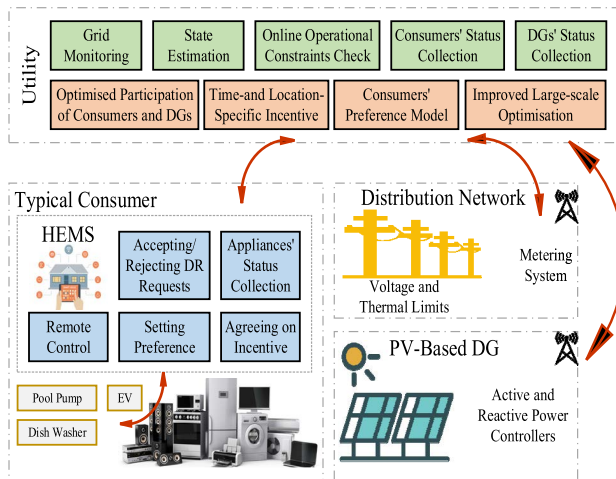


**FIGURE 1.** Architecture of the proposed voltage management system.

number of households are considered in the simulations assuming all appliances have the same power consumption rating of 1 kVA, and the impact of DR on network power loss at different times are not taken into account.

Therefore, in this paper, a dynamic incentive mechanism to compensate for such locational impact on DR implementation is developed to take into account the contributions of consumers in energy adjustment, voltage improvement, and power loss reduction. The weightings of these contributions are optimized here at different times considering the network situations.

Another challenge in DR implementation is to optimize the control of a large number of various types of household appliances through HEMSs simultaneously and maintaining the consumers' comfort levels by prioritizing their consumption preferences in addition to considering network constraints. Inappropriate load control may lead to network constraints violation [23] and unnecessarily increase the volume of load control which can cause discomfort to consumers and increase the DR cost. DR implementation through HEMSs and coordination of DGs, as proposed in this paper (as shown in Fig. 1) can benefit both utilities and consumers. All these considerations in the load control algorithm create a complex optimization process, which requires a long computational time. Various analytical and soft computing strategies such as heuristic approaches [24], reinforcement learning [25], etc., are proposed to solve such complex problems for scheduling appliances. Some of these approaches are successful in obtaining the optimal solution. However, they are not fast enough in convergence and entail heavy computational costs, which are not suitable for a fast voltage management process considering a large number of DR participants. Moreover, the consumption decision priorities of the individual DR participant to retain their comfort levels are important indices for a successful DR implementation, are not considered in the aforementioned studies.

The study in [6] provides a large percentage of real-time balancing reserve for the MV network by aggregating electric

water heaters (EWHs) for load shifting while maintaining the consumers' comfort levels. In [26], a virtual energy storage system concept is proposed considering EVs and ACs to cater for the comfort levels of consumers at different indoor temperatures. However, these studies are limited to control of few appliances. Multi-layers DR study in [27] uses only air conditioner (AC), EWH, and cloth dryer to satisfy both utility and consumer preferences. A load shedding optimization technique is proposed in [2] for the utility to maintain their network voltage considering a limited number of household appliances. These studies consider only a few selected appliances from a limited number of DR consumers in the load control, assuming all the consumers have similar appliances with fixed kW ratings of appliances without any fair optimized incentive distribution. In reality, the appliances' power ratings and their availability vary between the consumers and may not be the same across all participating consumers in a DR event. Therefore, a realistic approach considering the variability of household appliances and their different kW sizes for a large number of DR participants are yet to be investigated in the load control algorithm.

Toward this end, this study introduces a holistic multi-scheme load control strategy for managing multi-interval voltage fluctuations in the MV networks and minimizing the power loss with the following main contributions:

- 1) A dynamic incentive mechanism is proposed for fairly rewarding the DR participating consumers based on their energy contribution and their influence on the network voltage and loss improvements.
- 2) The load control algorithm is developed to optimize the DR participants' locations and support their consumption decisions to maintain their comfort levels by considering appliances' switching status, disturbance ratio and their fair interruption in the DR event.
- 3) An improved hybrid particle swarm optimization (IHPSO) algorithm is proposed in the load controller to provide fast and robust convergence in handling a large number of DR participants and objective parameters such as minimizing the network loss, DGs' reactive power contribution, DR cost and sizing, fair incentive distribution and the participants' consumption preferences.

The rest of the paper is organized as follows; Section II presents the proposed objective function, dynamic fair incentive strategy, multi-scheme DR for voltage management and consumer preference definitions and modelling. Section III explains the solution approach for the multi-interval voltage management. Section IV provides simulation results of the proposed approach, and the relevant conclusion is presented in Section V.

## II. METHODOLOGY

This section provides the details of the objective function and the proposed dynamic fair incentive rate design for the multi-scheme load control for different intervals of voltage management (as shown in Fig. 1).

**A. OBJECTIVE FUNCTION**

The optimization problem of each load control scheme has two conflicting objectives. The first objective is to satisfy the distribution network technical constraints including voltage magnitude, line thermal bounds, active power loss and DGs’ reactive power capabilities. The second objective is to provide fair incentive rates to consumers while minimizing the total cost of DR as well as consumers’ welfare disturbances. In the proposed optimization problem, the decision variables include the incentive rate factors of each DR candidate bus, the participating appliances’ switching variables and preferences, and the reactive power contribution from DGs. The outcomes of the optimization process are the optimal switching positions (ON/OFF) of the appliances, the fair incentive rates and the reactive power output of each DG at the time of each DR event. Thus, the objective function (OF) is formulated in the form of a mixed integer nonlinear programming problem.

$$\text{Min } [Of] \text{ } Of = \sum_{t=1}^T \left( P_{loss}^t \lambda^t + \sum_{i=1}^{N_{DR}^t} (DR_i^t \times \pi_i^t) + \sum_{k=1}^{N_{DG}} (Q^{k,t} \times \eta_k) \right) \Delta t + Penalty_{Total} \quad (1a)$$

where,  $DR_i^t = \sum_{n=1}^{N_A^t} |An_i^t| \times P_i^{n,t}$ ;

$$Penalty_{Total} = Penalty_{Volt.violation} + Penalty_{Power\ loss} + Penalty_{switching}^t \quad (1b)$$

$$s.t. V_{min} \leq V_j^t \leq V_{max}, \forall j, t \quad (1c)$$

$$|I_j^t| \leq I_{max}, \forall I, t \quad (1d)$$

$$Q_{min}^{k,t} \leq Q^{k,t} \leq Q_{max}^{k,t} \forall k, t \quad (1e)$$

Here,  $DR_i^t$  represents the total kW DR contribution from  $i^{th}$  candidate at  $t^{th}$  timeframe of a DR event;  $\lambda^t$  and  $\pi_i^t$  present the energy cost from the upstream grid and the associated incentive rate (\$/kWh) from the corresponding DR bus;  $\eta_k$  is the price of reactive power generation by DGs (\$/kVAr);  $N_{DR}^t$  is the total number of DR candidate consumers participating in a DR programming at time  $t$ ;  $\Delta t$  is the time frame duration of a DR event;  $T$  represents the number of time intervals for DR events in a particular day;  $P_{loss}^t$  is the total network active power loss at time  $t$ .  $An_i^t$  is the optimised switching status (ON/OFF) of the  $n^{th}$  appliance of the  $i^{th}$  consumer at time  $t$  during a DR event.  $P_i^{n,t}$  is the rated kW demand of the  $n^{th}$  appliance participated in the DR event.  $N_A^t$  is the total number of appliances of a consumer considered in a DR event. The total kW for DR contribution ( $DR_i^t$ ) from  $i^{th}$  candidate location is calculated by aggregating all kW ratings of participating appliances at time  $t$ . The limits of the magnitude of bus voltages, line thermal limits and reactive power output of DGs are expressed in (1b)-(1e), respectively. The reactive power output of each DG is minimized by the formulation of OF so that the maximum capacity

of the DGs can be used for active power production. The DR cost for each participating consumer is then calculated by multiplying the total controlled demand (kW), optimized incentive rate (\$/kWh) of the corresponding bus (as explained in Section II.B), and the duration (in hours) of the DR event. The  $Penalty_{Total}$  factor is a combination of voltage violation penalty factor ( $Penalty_{Volt.violation}$ ), power loss penalty factor ( $Penalty_{Power\ loss}$ ) and appliances’ switching constraints penalty factor ( $Penalty_{switching}^t$ ). These applied penalty factors will be discussed in Sections II.D and IV. In the following, the DR incentive rates and the associated contribution will be calculated.

**B. THE INCENTIVE RATE ALLOCATION AND DR LOCATION SELECTION**

Use DR participants based on their locations in the network will have a higher influence on the network parameters (such as bus voltages, line currents, and network loss) and are tended to be interrupted more in a DR event than those participants located comparatively less sensitive locations in the same network [21], [22]. As a consequence, DR participants located in the buses with higher impacts on the network parameters, contribute more to the voltage and loss improvements than the other participants. If all the participating consumers are provided with an equal incentive rate (\$/kWh) (e.g., as considered in [12], [25], and [28]), it implies a potential fairness issue on the incentive distribution between the participating consumers. To provide a better balance between the contributions and the rewards to the participating consumers, this study proposes a mechanism of calculating incentive rate dynamically for each DR event, which uses the location of the participating consumers in the network, technical parameters of the network and the time of the DR event. The calculated incentive rate of each participant is mainly a combination of three components: energy cost rate (\$/kWh) based on the time of use (TOU) tariff, voltage improvement cost and total loss improvement cost, as shown in (2a). As seen in (2a),  $k_1^t$ ,  $k_2^t$  and  $k_3^t$  are the coefficient factors of energy cost, voltage improvement cost and total power loss improvement cost, respectively, which are optimized dynamically at the time of DR consumers’ participating in a DR event (discussed in Section IV). The proposed algorithm will optimize these coefficients for each DR bus based on the voltage and power loss sensitivities and applied penalty factors for voltage and power loss violations (as explained in Section IV) to determine the incentive rate of each DR bus. The objective function in (1a) will try to minimize the total cost by optimizing  $k_1^t$ ,  $k_2^t$  and  $k_3^t$  values. Equations (2b)-(2c) and (2d)-(2e) are used to calculate voltage and total loss improvement factors of each selected DR bus for rate design, respectively.

$$\pi_i^t = TOU_i^t \times \left( k_1^t + k_2^t \times \Delta V_i^t + k_3^t \times \Delta P_{loss}^{i,t} \right), \quad \forall i, t, \sum k^t = 1 \quad (2a)$$

$$s.t. \Delta V_i^t = \frac{AVS_i^t}{\frac{1}{N_{DR}^t} \sum_{i=1}^{N_{DR}^t} AVS_i^t}, \forall i, t \quad (2b)$$

$$AVS_i^t = \frac{1}{N_v} \sum_{j=1}^{N_v} \frac{\partial |V_j^t|}{\partial P_i^t}, \forall i, t \quad (2c)$$

$$n\Delta P_{loss}^{i,t} = \frac{TLS_i^t}{\frac{1}{N_{DR}^t} \sum_{i=1}^{N_{DR}^t} TLS_i^t}, \forall i, t \quad (2d)$$

$$TLS_i^t = \frac{\partial |P_{loss}^t|}{\partial P_i^t}, \forall i, t \quad (2e)$$

$$P_{loss}^t = \sum_{l=1}^{N_l} R_l |I_l^t|^2, \forall l, t \quad (2f)$$

where,  $AVS_i^t$  represents the average of sensitivity factors in all voltage violated buses ( $N_v$ ) due to power change ( $\partial P_i^t$ ) at  $i^{th}$  bus at  $t^{th}$  time interval.  $(\partial |V_j^t|)$  is the voltage change at each violated bus  $j$  at time  $t$  due to power change ( $\partial P_i^t$ ) at  $i^{th}$  bus, which is obtained from inverse Jacobian matrix [9]. The buses with the higher  $AVS_i^t$  values are considered for ranking the DR candidate buses.  $TLS_i^t$  represents the sensitivity factor of total active power loss ( $\partial |P_{loss}^t|$ ) with respect to power change ( $\partial P_i^t$ ) at  $i^{th}$  bus at  $t^{th}$  time interval. The bus with higher loss sensitivity ( $TLS_i^t$ ) value has more influence on total network loss change due to active power change in that bus [30].  $N_l$  is the number of branches,  $I_l^t$  is the current flowing through branch  $l$  at time  $t$ ,  $R_l$  is the resistance of branch  $l$ . As seen, branch current is involved in DR selection process for the purpose of reducing thermal limit violations in a network, so, another index for current is not defined here. These sensitivities are calculated in accordance with the proposed approach in [30] to determine the DR candidate buses. The candidate locations for DR implementation are crucial for the MV networks, as there are many consumers connected in each bus of the MV networks. Identifying the effective locations for DR implementation which have high influences on the network voltage and loss improvement, will reduce the optimization search space and time, total DR implementation size, consumer disruptions, and consequently the total DR cost [9]. It is important to mention that sensitivity analysis is conducted with respect to active power changes from participating consumers, as many policies at the moment recognize energy contribution of small-scale consumers in DR programs [9]. Therefore, to identify the optimal DR candidate locations for each DR event, in this study, sensitivity analysis for both voltage and total power loss in regard to active power changes are performed. The combination of the bus voltage sensitivity in (2c) and the total power loss sensitivity in (2e) is considered to rank each bus of the network for DR candidate bus selection. The bus with the highest summed value of (2c) and (2e) will be ranked as 1, with the second highest value, ranked 2, and so on. Section IV provides the bus ranking results using the combined approach of voltage and power loss sensitivities. The typical TOU

electricity pricing structure for the proposed incentive rate development is obtained from [29].

### C. MULTI-SCHEME LOAD CONTROL FOR VOLTAGE MANAGEMENT

The proposed load control algorithm is implemented into two DR schemes i.e., 10-minute and 2-hour schemes for handling the short and long intervals of voltage variations in the MV networks, respectively. Household appliances are categorized based on their operation cycles to use in each DR scheme, as discussed below.

#### 1) SHORT-INTERVAL (10-MINUTE) DR SCHEME

A maximum of 10-minute load control is considered in this scheme for the short duration cloud movements. The candidate appliances for this DR scheme are AC and EWH. These devices can be interrupted for a maximum of 10-minute of their control cycle to avoid consumer discomfort and rebound effect of DR. Thus, they can be interrupted multiple times to compensate for the fast variations of voltage in the network due to the cloud transients. To minimize the consumer discomfort and DR rebound effect, once the load control signal is sent to these devices, another signal will not be sent to these devices for the next 10 minutes. The switching ON and OFF decisions of available ACs and EWHs in each DR candidate bus in a DR event depend on their thermostat set points and dead band temperatures [6], [21].

#### 2) LONG-INTERVAL (2-HOUR) DR SCHEME

A maximum of 2-hour load control is reasonable for managing long interval voltage variations caused by the solar PV generations [31]. In this scheme, we have selected those electric household appliances that have lower impacts on the consumers' comfort levels if their operation is deferred and have flexibilities to shift their operation time. Appliances like dishwasher, washing machine, pool pump, dryer, and EV are suitable for this scheme. For dishwasher and washing machine, the consumption cycles have to be completed once started their operation. However, their operating/starting time can be shifted. Appliances like EV, pool pumps and smart dryer [32] can be interrupted during their operation cycles and thus can be interrupted any time during DR events.

### D. CONSUMER CONSUMPTION PREFERENCES IN DR EVENT

DR participants' consumption preferences are taken into account in both of the above mentioned DR schemes, as described below. Utility collects the DR appliances' consumption preferences from each participant consumer prior to any DR activation, which will minimize the consumer comfort violations. Two important criteria are considered in this paper to model the consumer preferences:

- 1) consumption preferences on each DR appliance, and
- 2) each DR appliance's switching constraints.

TABLE 1. Parameters for appliance consumption preferences.

| Preference | Definition (mode) | Initial status and controllable condition         | Controllable in DR event? | $An_i^t$ |
|------------|-------------------|---|---------------------------|----------|
| 0          | not restricted    | the appliance is OFF and it can be switched ON    | Yes                       | 1 or 0   |
| 1          | not restricted    | the appliance is ON and it can be switched OFF    | Yes                       | -1 or 0  |
| 2          | not available     | the appliance is not currently available for DR   | No                        | 0        |
| 3          | priority          | the appliance is ON and it cannot be switched OFF | No                        | 0        |
| 4          | restricted        | the appliance is OFF and it cannot be switched ON | No                        | 0        |

1) CONSUMPTION PREFERENCES

The consumption preferences of each DR appliance are defined as consumption restriction and priority. During a DR event, these appliances will not be switched ON or OFF. In Table 1, the numerical values (0 to 4) are considered to define the initial switching statuses and consumption preferences of each appliance in the load control algorithm prior to activate in a DR event. The switching status of  $n^{th}$  appliance of the  $i^{th}$  consumer is defined by  $An_i^t$ , as shown in (3).  $An_i^t$  is a decision variable in the optimisation process for finding an optimal load adjustment in a DR event (discussed in the next section). Appliances allocated with the preference of 2, 3 or 4 (as shown in Table 1) by the consumers, will not be included in the optimization process and their switching status (ON/OFF) will be unchanged during the optimization process. Thus, the corresponding  $An_i^t$  is always zero. Based on  $An_i^t$  value for each appliance, the proposed load control algorithm tries to minimize the voltage violations in the distribution network, comfort disturbances, and the DR cost, as discussed in Section II.A.

$$An_i^t = \begin{cases} 1 & \text{the appliance is turned ON} \\ 0 & \text{no change is occurred} \\ -1 & \text{the appliance is turned OFF} \end{cases} \quad (3)$$

2) APPLIANCE SWITCHING CONSTRAINTS

In addition to considering appliances' consumption preferences, the load control algorithm minimizes the random switching of appliances in a DR event. This avoids switching ON/OFF of large number of appliances as a result of reduced disturbances on the consumer comfort levels. In order to tackle this optimization problem, two constraints are applied in the load control algorithm for each participating appliance in a DR event, which are 1) assigning a priority to those appliances which have high kW power ratings to be controlled first, 2) limiting the excessive amount of appliances control of each consumer. By applying the above constraints on the participating appliances, a less amount of load adjustment is likely required for each DR event as well as consumer inconveniences will be minimized.

To comply with the appliance control priorities and minimize the excessive switching disturbances on a consumer's appliances, the average disturbance ratio (ADR) factor is

proposed in this paper. ADR represents the ratio of the total demand change ( $\Delta P$ ) to the total number of disturbed appliances of  $i^{th}$  consumer at  $t^{th}$  time interval, as in:

$$ADR_i^t = \frac{\Delta P_{ADR(i)}^t}{\sum_{n=1}^{N_A} |An_i^t|} \quad (4a)$$

$$s.t. \Delta P_{ADR(i)}^t = \left| \sum_{n=1}^{N_A} An_i^t \times P_i^{n,t} \right| \quad (4b)$$

where  $\Delta P_{ADR(i)}^t$  is the sum of kW demand change,  $N_A$  is the total number of appliances of a consumer participating in a DR event,  $P_i^{n,t}$  is the rated kW demand of the  $n^{th}$  appliance. All the parameters are for the  $i^{th}$  consumer at  $t^{th}$  time interval during the DR event. ADR is treated as a technical constraint during the optimisation process in the objective function (in Section II.A). The associated penalty factor for  $ADR_i^t$  presented in (5), is added into the objective function (1a).

$$Penalty_{ADR_i^t} = \begin{cases} \mathcal{M} & \mathcal{P}_1 \geq ADR_i^t \\ \mathcal{M} (2 - ADR_i^t) & \mathcal{P}_1 < ADR_i^t < \mathcal{P}_2 \forall i, t \\ 0 & \mathcal{P}_2 \leq ADR_i^t \end{cases} \quad (5)$$

According to (5), the penalty factor of  $ADR_i^t$  is maximum when  $\mathcal{P}_1$  greater than or equal to  $ADR_i^t$  to exclude the corresponding switching solution from the load control optimisation search space.  $\mathcal{M}$  is a large number (i.e. =  $10^2$ ) which is implemented in order to eliminate the unappropriated switching solutions. If  $ADR_i^t$  value is larger than or equal to  $\mathcal{P}_2$ , the penalty factor is zero to relax the  $ADR_i^t$  constraint. If  $ADR_i^t$  is confined within  $\mathcal{P}_1$  and  $\mathcal{P}_2$ , a descending linear equation is implemented to provide a linear relationship between the value of ADR for each participant and the penalty factor. To clearly understand the  $ADR_i^t$  constraint, let us consider a consumer have a 2kW washing machine and 1kW pool pump, which current switching status are OFF and ON, respectively. During a DR event, if the optimization algorithm decides to switch on the washing machine but keep the switching status of pool pump unchanged (which is ON), according to (4a) and (4b), the ADR value will be 2 (=2/1). However, if the optimization algorithm decides to switch on the washing machine and switch off the pool pump at the same time, the ADR value will be 0.5 (|2 - 1|/2). Higher the ADR value, less penalty factor will be added into the objective function in (1a). The  $\mathcal{P}_1$  and  $\mathcal{P}_2$  values are user defined based on the required optimisation output and maximum and minimum kW ranges of the participated appliances. In this study we considered  $\mathcal{P}_1$  and  $\mathcal{P}_2$  values are 2 and 0.5, respectively. As a result, the  $ADR_i^t$  constraint in (4a) helps the load control algorithm by selecting the large (kW) available appliances of the DR participant to be controlled in a DR event and thus, reduces the random switching of the appliances.

Further, to limit an excessive amount of appliances control for some participated consumers in a DR event, an additional constraint called appliance fair interruption (AFI)

is added into the optimization process. As stated before (in Section I), some consumers are usually interrupted more than others due to their sensitive locations in the network. If this constraint is not included in the algorithm will create a fairness issue regarding the number of appliance interruptions in a DR event. To limit the excessive number of appliances interruption for some location-based consumers, AFI will be calculated and minimized by the proposed load control algorithm in each DR event. AFI is defined using (6a) as the total number of disturbed appliances for each consumer. The associated penalty factor for AFI treated as a constraint in the optimization, is shown in (6b).

$$AFI_i^t = \sum_{n=1}^{N_A} |An_i^t|, \forall t, i \quad (6a)$$

$$Penalty_{AFI_i^t} = \begin{cases} \mathcal{M}(AFI_i^t - 2), & AFI_i^t > T_1 \text{ (long term)} \\ \mathcal{M}(AFI_i^t - 1), & AFI_i^t > T_2 \text{ (short term)} \\ 0, & \text{else} \end{cases} \quad (6b)$$

where  $AIFI_i^t$  is AFI for  $i^{th}$  consumer at  $t^{th}$  time.  $Penalty_{AFI_i^t}$  is applied in the objective function (OF) stated in Section II.A for both long- and short-interval DR when  $AFI_i^t$  value for  $i^{th}$  consumer is greater than  $T_1$  (i.e. = 2 appliances) and  $T_2$  (i.e. = 1appliance), respectively.

Finally, the total penalty factor ( $Penalty_{switching}^t$ ) is defined as follows:

$$Penalty_{switching}^t = \sum_{i=1}^{N_{DR}^t} Penalty_{ADR_i^t} + Penalty_{AFI_i^t} \quad (7)$$

### III. SOLUTION APPROACH

The proposed voltage management strategy coordinates with consumers' load control and DGs' reactive power contributions in each DR scheme for effective voltage management in the distribution networks, while maintaining the consumption preferences and fair incentives to the participants.

Fig. 2 illustrates a flowchart of the proposed voltage management method. It shows that each day the utility updates the forecast of the DGs' output power and load demand, e.g., for a span of 2 hours in advance using available reliable forecasting tools [33] and run offline load flow for every 5 minutes of this time span to check the network voltage level limits. Fig. 2 shows that the offline load flow study with the forecasted data for voltage violation identification is achieved within 1 minute. Once the buses with voltage violations are identified, the DR scheme (either short- or long-interval) is selected in step 2 considering the duration of the voltage violation based on the 5-min load flow analysis. After the selection of a DR scheme, network buses are ranked using (2c) and (2e) within 25 to 30 seconds. The consumers located at the identified buses are then notified about the DR event. Upon this receiving notification, interested consumers can update their existing consumption preferences if they

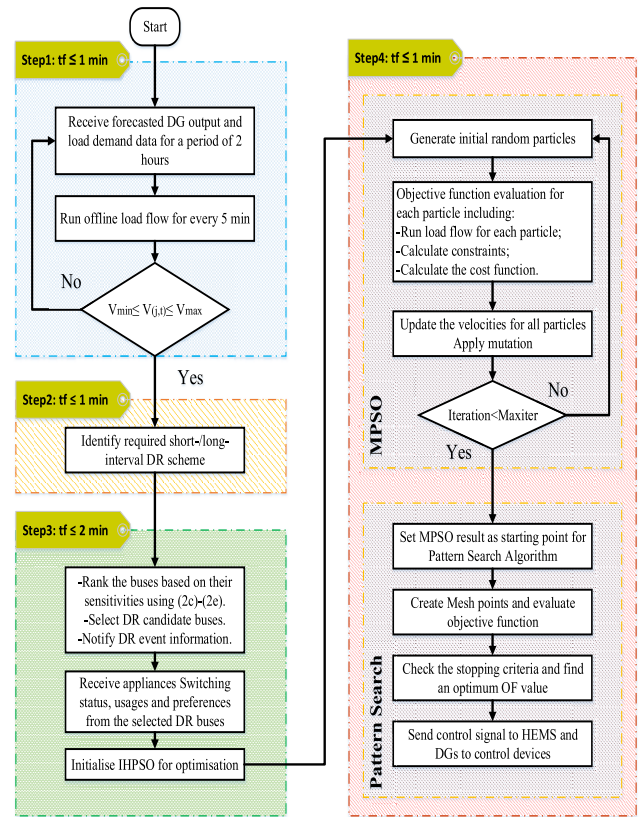


FIGURE 2. The flowchart of the proposed voltage management method, **tf**: time frame.

wish. Consumers who signed for participation in any DR scheme need to provide their lists of available DR appliances to the utility. Consumers can predefine their consumption preferences for each day through HEMSs. Furthermore, the consumers have an opportunity to change their preferences frequently before committing their participation in any DR event. The information exchange with the consumers takes less than a second using the technologies like WiMAX (with a bit rate of 5 to 25Mbps) and ZigBee (with a bit rate of 250 kbps) [12]. Therefore, the total required time for step 2 is less than 1 minute.

In step 3, participated consumers' information such as appliances' current states, consumption preferences and previous history of DR event participations are collected. Data collection and processing in this stage are achieved within 2 minutes. The final step 4 optimizes the objective function to calculate the optimum switching positions of the appliances, DGs' reactive power contributions and fair dynamic incentive rates to the participated consumers to calculate the total DR cost. Once the optimum solution is obtained, the control signals are sent to appliances and DGs' inverters to switch ON/OFF, and provide reactive power support, respectively. This stage is estimated to be performed within 2 minutes, as the average computational time of the optimization process for long- and short-interval schemes are around 50 and 20 seconds in the IEEE 33-bus system respectively using MATLAB software on Intel CORE i7-2600 PC with a clock speed of

3.4 GHz and 12GB RAM. The next section describes the optimization process based on the modified hybrid PSO.

#### A. IMPROVED HYBRID PARTICLE SWARM OPTIMISATION (IHPSO)

To solve the complex non-linear objective functions (as mentioned section II.A), a Particle swarm optimization (PSO) algorithm is proposed in this study. Various analytical and soft computing methods such as Learning Automata [34], Reinforcement Learning with Q-learning [35] and Evolutionary Algorithm (EA) [36] are previously being used to address the complex problems of scheduling DR appliances. In some studies, like [17], [18], [19] propose bi-level metaheuristic-based algorithm and interval analysis methods to address complex planning problem for solving voltage and power loss issues in the microgrids. Though these metaheuristic-based algorithms are suitable in addressing complex problems, with the increased number of optimization variables they may increase the computational burden and time and may not provide optimum outcomes. The PSO algorithm is one of the derivative-free heuristic algorithms, which has the proven ability to provide fast convergence with robust output and require less computational time for the large scale non-linear and mixed integer problems [13], [37]. The main benefits of using PSO algorithm are that it has robust control parameters and computational efficiency as compared with the mathematical algorithm and other heuristic optimization techniques [38]. It has fewer parameters to adjust and constraints acceptance and thus, it is easy to implement.

In this paper, an improved hybrid PSO is proposed which is based on a modified version of classical PSO [13] incorporated with a pattern search (PS) algorithm [39] for providing fast convergence and robust optimization output to solve the voltage management problems. In this approach, PSO is responsible for the exploration of the search space and the detection of the potential regions with optimum solutions, while PS is used to produce effective exploitation on the potential regions obtained by PSO. An important drawback of the PS method is the need to supply a suitable initial point [39]. Where PS hybrids with PSO algorithm, the initial starting point will no longer needs to be specified by the user, it will be automatically generated by the PSO phase. However, the standard PSO may not provide a suitable initial starting point for PS in high dimensional problems, as the standard PSO sometimes converges into local optima resulting in low optimizing precision. In order to improve the accuracy of the solution, in this study, a mutation function is applied in the standard PSO particle update rules. The mutation function is conceptually equivalent to the mutation in genetic algorithms (GA) [13]. A comparison study in [38], shows that this modified version of PSO (MPSO) outperforms other heuristic methods such as the original PSO, GA, and simulated annealing in terms of accuracy, robustness and speed. Furthermore, the constriction factor approach is adopted in PSO in addition to the mutation method, which outperforms compared to inertia weight approach [38].

Therefore, an improved hybrid PSO (IHPSO) is proposed in this study as a combination of MPSO and PS algorithms to improve the optimisation performance and minimise the computational time. Although the standard PSO combined with PS is discussed in [39], we propose a hybrid model of MPSO with PS in this paper with higher capabilities in finding better solutions in a short period of time. In this hybrid method, MPSO runs first to find the near global best location. This global solution is provided to PS for further minimisation of the objective function. The idea behind this strategy is to let MPSO utilise its strength aggressively exploring the search space to find near optimum solution, then let PS utilises its strength to quickly find the global optimum solution by searching locally around the solutions given by MPSO. Fig. 2 shows the hybrid optimisation process with the MPSO and PS algorithms in Step 4.

The velocity and position updates of each MPSO particle at iteration  $k$  to search for the optimal solution are as follows:

$$\begin{aligned} V_i^{k+1} &= \gamma \times (V_i^k + 0.5 \times \varphi_{max} \times rand \times (P_{best_i} - X_i^k) \\ &\quad + 0.5 \times \varphi_{max} \times rand \times (G_{best} - X_i^k)) \\ X_i^{k+1} &= X_i^k + V_i^{k+1} \end{aligned} \quad (8a)$$

where  $V_i^k$  and  $X_i^k$  are velocity and position vectors of  $i$ th particle at iteration  $k$ , respectively;  $\gamma$  is the constriction factor coefficient;  $P_{best_i}$  is the best value vector of  $i$ th particle so far;  $G_{best}$  is the best value among  $P_{best_i}$  so far; and  $rand$  is a random number generator uniformly distributed between 0 and 1. The constriction factor coefficient ( $\gamma$ ) is calculated as shown in (8b).  $\varphi_{max}$  and  $\varphi$  are constant values. In this study  $\varphi_{max} = 4.05$  and  $\varphi = 1$  are considered [13].

$$\gamma = \begin{cases} \sqrt{\frac{2\kappa}{\varphi - 2 + \sqrt{\varphi^2 - 4\varphi}}}, & \varphi > 4 \\ \sqrt{\frac{\kappa}{\varphi}}, & else \end{cases} \quad (8b)$$

In (8b),  $\kappa \in [0, 1]$  is a coefficient that allows control of exploration versus exploitation propensities. For a bigger value of coefficient  $\kappa$ , particles desire more exploration and preventing explosion, derives slow convergence and searching thoroughly the space before collapsing into a point. However, for smaller values, particles care more exploitation and less exploration. The mutation function is applied when  $G_{best}$  is not improving while the increasing of number of iterations. The mutation function selects a particle randomly and then adds a random perturbation to a randomly selected element of the velocity vector of that particle by a mutation probability. In this paper, if the  $G_{best}$  after 11 iterations is not improving, the mutation function with the mutation probability of 0.85 is applied.

MPSO handovers its global best ( $G_{best}$ ) location to PS as an initial point ( $X_0$ ), which has a great influence on PS's calculation results. PS utilizes a set of directions comprising a "pattern" that it uses to search around the initial point ( $X_0$ ) to find better points and ignores the rest of the search space. This



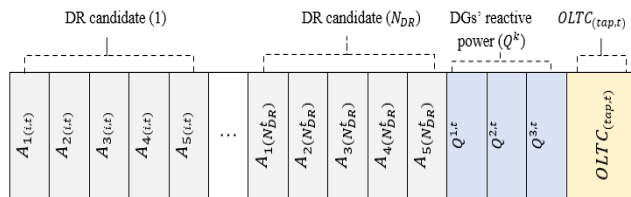


**FIGURE 3.** IHPSO particle structure for voltage management using DR coordinated with DGs and OLTC.

allows PS to find the optimum solution with much greater efficiency. PS finds a series of points  $X_0, X_1, X_2, \dots, X_n$ , which are closer and closer to the optimal value of points. When the termination conditions are met, the last point will be the final solution for this search. In this study, the mesh size and the mesh expansion and constriction factor are selected as 1, 2 and 0.5, respectively. As for the stopping criteria, all tolerances are set to  $10^{-6}$  or reaching the maximum number of iterations. The formulation details of MPSO and hybrid of the standard PSO with PS algorithm are presented in [13] and [39], respectively.

In this study, each particle in IHPSO is composed of a number of cells that represent as decision variables in the optimization. As an example, Fig. 3 shows the coordinated approach of DR with three DGs ( $Q^k$ ) and on-load tap changer ( $OLTC_{tap}$ ) for the long-interval DR scheme. In the long-interval DR scheme (as explained in Section II.C), a maximum number of five appliances of each candidate consumer are considered for DR participation. Each of these appliances is defined with five switching control variables (as mentioned in Table 1). Therefore, the number of cells (variables) for the total DR candidate ( $N_{DR}$ ) is  $5 \times N_{DR}$ , representing  $A_{n(i,t)}$  for  $n = 1, \dots, 5$  and  $i = 1, \dots, N_{DR}$ . Three cells (variables) are defined for three DGs. If more voltage regulator devices are required to add in the optimisation (e.g., OLTC control is added into the optimization process, as discussed in Section IV.F) based on the number of variables of the device to be optimized, the number of cells will be added into each particle of IHPSO which show great flexibility and scalability of this proposed approach. For example, in Fig. 3, one cell is added for OLTC tap variable. Section IV.F presents the optimized results with DR coordinated with DG and OLTC in the IEEE 69-bus system.

To accelerate the optimization process with IHPSO, the direct load flow method [40] is used in this study to calculate the network parameters including  $V_{(j,t)}$ ,  $I_{(l,t)}$ , and  $P_{T.loss(t)}$  for each particle at every iteration. This load flow approach uses the bus injection to branch current (BIBC), branch current to bus voltage (BCBV), and distribution load flow (DLF) matrices which are implemented in MATLAB for this purpose.

**IV. SIMULATION RESULTS AND CASE STUDIES**

This section provides simulation results for two DR schemes (i.e., long- and short-interval schemes) considering several worst scenarios to show the effectiveness of the proposed

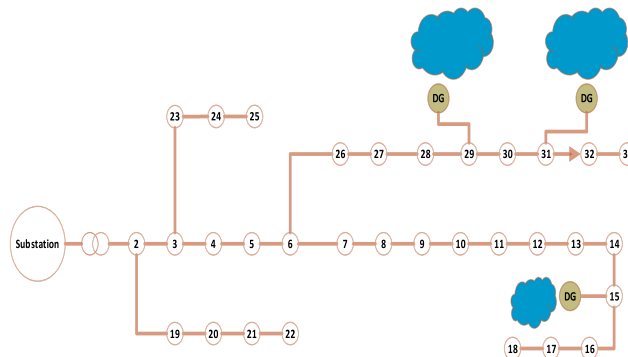


**FIGURE 4.** IEEE 33-bus MV network with multiple DG connections.

voltage management method. The proposed approach is tested on an IEEE 33-bus radial distribution test system shown in Fig. 4. In this paper, the IEEE 33-bus distribution system is modified with three large solar PV-based DGs with a capacity of 1.22 MW each connected to buses 15, 29, and 31. The optimal locations of the DG units in the 33-bus distribution network as shown in Fig. 4 are identified by the study in [41]. To analyze the DG power output, 1-minute interval power production data is gathered for a 1.22 MW PV system located at the University of Queensland’s St Lucia campus in Brisbane [42], [43]. In this study, it is assumed that a total 90 consumers are available to participate in each DR event and randomly distributed in the DR candidate buses. In this study, the permitted boundary of voltage magnitudes for all network buses is considered within  $\pm 5\%$  of nominal voltage [9]. In addition, the amount of reactive power and active power from each DG unit can be obtained by considering the limits of power factor ( $PF_i$ ) within  $[-0.95, +0.95]$ .  $P_1$  and  $P_2$  are 0.5 kW and 2 kW, respectively (as discussed in Section II.D). The total number of PSO particles is considered 300 and a self-adaptive iteration size technique is taken into account. The mutation probability for MPSO is considered 0.85. As discussed previously, the proposed dynamic fair incentive mechanism implemented through large-scale consumer participation is a new approach compared to the previous methods [44], [45].

**A. CASE 1: LONG-INTERVAL VOLTAGE VARIATION**

Case study 1 includes two scenarios of long-interval voltage variations in the IEEE 33-bus network. Fig. 5 depicts the load profile and the PV-based DG power output for a typical hot summer day. Fig. 5 also presents the maximum voltage drops at far end buses of the network caused by significant DGs’ output power drops during 11:15 to 12:08 (53 minutes) and during 13.09 to 14.19 (70 minutes). As shown, voltages at some remote buses fall extremely low below the standard limits. Two DR events are applied to improve these long-interval voltage variations using the proposed voltage management procedure in Fig. 2. These two DR events are shown in Fig. 5, as listed below:

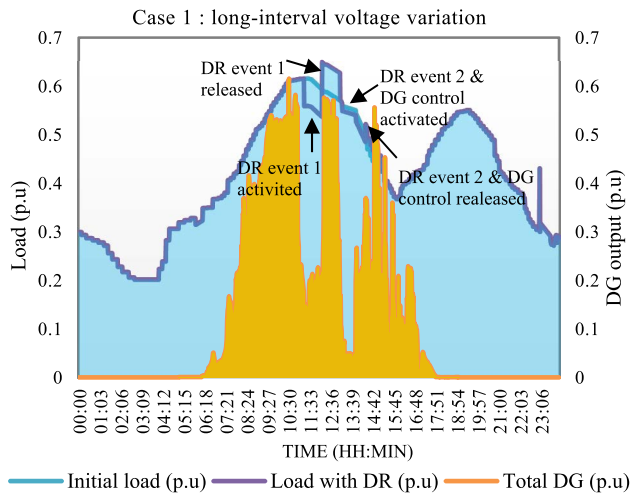


**FIGURE 5.** Load and DG power output profile with and without DR deployment.

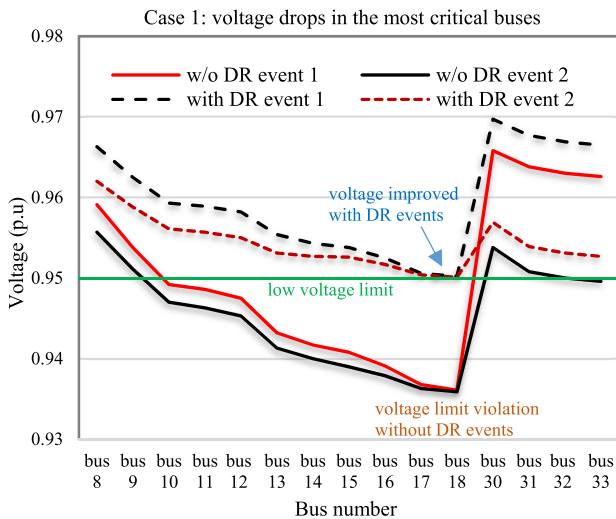


**FIGURE 6.** Voltage profiles of critical buses with and without (w/o) DR deployment.

Due to the prolonged voltage variations in the network caused by the slow cloud movement, the 2-hour DR scheme is initiated for each DR event to solve the under voltage problems. As seen in Fig. 5, the DR event 1 is activated from 11:15 to 12:08, which reduces the initial load demand (2,828 kW) by about 10%. The DR event 2 is initiated at 13:09 and remained active for around 70 minutes, which reduces the initial load demand (2,600 kW) by 8.6% and injects a total 66 kVar from DGs into the network. The improvement of voltage profiles during DR events 1 and 2 are presented in Fig. 6, which shows the effectiveness of the proposed approach in managing voltage violations during slow cloud movement. DR event 1 for the event during 11:15 to 12:08 (53 minutes), DR event 2 for the event during 13.09 to 14.19 (70 minutes).

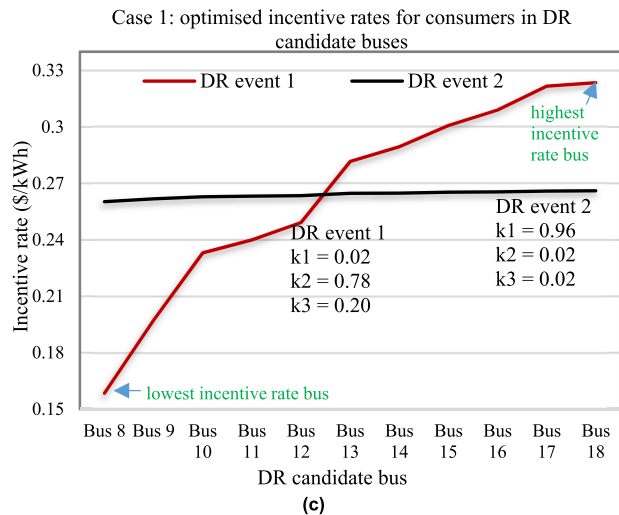
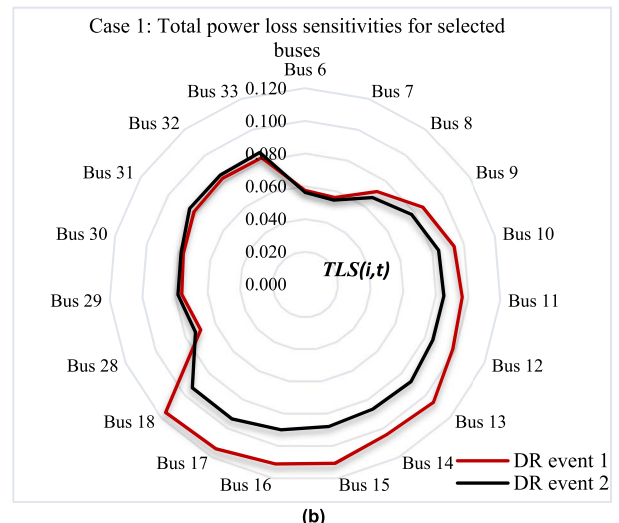
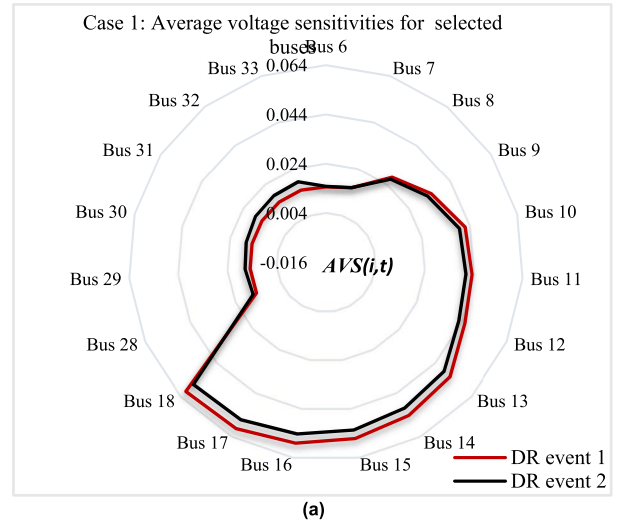


**FIGURE 7.** (a) Average voltage sensitivities for selected buses, (b) total loss sensitivities for the buses, and (c) optimized incentive rates for consumers in DR candidate buses.

Figs. 7(a) and 7(b) show the average voltage sensitivity ( $AVS_{(i,t)}$ ) and total power loss sensitivity ( $TLS_{(i,t)}$ ) with respect to active power change in each voltage violation bus

in order to identify the DR candidate buses (as explained in Section II.B). As seen, the voltage and total loss sensitivity values are much higher for the remote buses 8 to 18 in respect to active power changes in those buses. Therefore, the combined sensitivity values for buses 8 to 18 are higher than other buses in the network. Thus, these 11 buses are considered as DR buses for both DR events 1 and 2. Fig. 7(c) illustrates the optimized incentive rates (\$/kWh) for each DR candidate bus obtained from (2a). It can be seen that for DR event 1, the incentive rate increases progressively from bus 8 to bus 18. It is due to the far end buses (i.e., 16, 17, and 18) have higher voltage and loss sensitivities and they contribute more to voltage and loss improvements. Thus, the corresponding consumers in those buses will receive higher incentive rates as compared to the low sensitive buses, which shows a fair incentive rate distribution among the DR participants. The optimized voltage improvement coefficient  $k_2$  is higher than the loss coefficient  $k_3$  for DR event 1. It is due to our primary goal is to improve the network voltages, which is prioritized by adding higher voltage violation penalty cost ( $Penalty_{Volt.violation}$ ) than the power loss penalty cost ( $Penalty_{Power loss}$ ) in the objective function (1a). The utility can adjust the penalty factors for the voltage and power loss based on the network conditions and can priorities one power loss over voltage violations.

Interestingly, for the DR event 2, the optimized incentive rates for buses 8 to 18 do not have much differences, it is due to the fact that the coordinated control of reactive power of DGs in the DR event 2 reduces the incentive rates in DR candidate buses. In the DR event 2, the coordination control of reactive power of DGs with DR event is used due to only load control of consumers is not sufficient to manage the voltages in all buses. The reactive power injected from the DGs into the network improves the bus voltages and reduces network losses. As a result,  $k_2$  and  $k_3$  values in DR event 2 are much lower compared to DR event 1, as shown in Fig. 7(c). The  $k_2$  and  $k_3$  values are related to voltage improvement factor and power loss improvement factor, respectively (as explained in Section II.B). The optimized values of these parameters are location dependent, mainly depend on the voltage and power loss sensitivities. Table 2 shows the optimized results of some important variables from the proposed voltage management algorithm applied in DR events 1 and 2. It can be seen that the total penalty factor is zero for both DR events, which means the consumers' consumption preferences, appliances' switching constraints (as discussed in Section II.D) and bus voltage constraints ( $\pm 5\%$ ) are maintained to minimize the consumers' comfort violation and voltage violation. As shown in Table 2, in DR event 2, the three DGs provided different reactive power levels. It is interesting to note that the amount of the reactive power injection varies based on the location of the DGs in the network. According to the Figs. 7(a) and 7(b), the voltage sensitivity and power loss sensitivity are higher in bus 15 than bus 31 and bus 29, in where the three DGs are connected respectively. As a result, the DG located in bus 15 provided

TABLE 2. Results of case 1 using the proposed voltage management approach (VMA).

| DR event | no VMA       | After VMA implementation (optimized values) |         |                  |                |   |
|----------|--------------|---|---------|------------------|----------------|---|
|          | $P_{T,loss}$ | $P_{T,loss}$ (kW)                           | DR (kW) | $DR_{cost}$ (\$) | Penalty (kVAr) | DG OF (\$)  |
| 1        | 62.3 kW      | 44.7  | 261     | 67.3             | 0              | 111.9<br>DG <sub>15</sub> =28                         |
| 2        | 83.1 kW      | 61.1  | 222.4   | 58.8             | 0              | 139.8<br>DG <sub>29</sub> =16<br>DG <sub>31</sub> =22 |

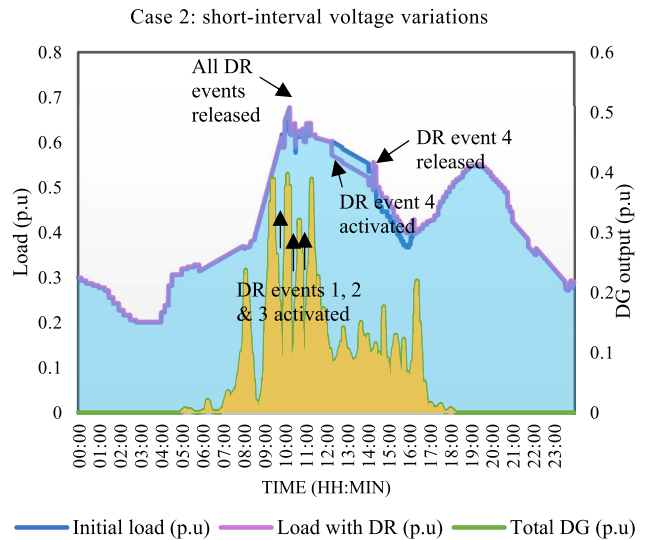


FIGURE 8. Load and DG power output profile with and without DR deployment.

more reactive power support as compared to DGs located in buses 29 and 31 to reduce the voltage violation and power loss in the network.

### B. CASE 2: SHORT-INTERVAL VOLTAGE VARIATIONS

Fig. 8 presents a typical day where high variability of PV-based DG power generation is occurred due to the fast-moving clouds. The cloud transient created large changes in the net load and caused voltage drops in some remote buses, as shown in Fig. 9. To compensate for the voltage drops due to intermittent DG power generations, four DR events are initiated as below, in which DR events 1 to 3 are short-interval and DR event 4 is a long-interval DR:

- 1) DR event 1 for the event during 09:50 to 09:57 (7 minutes),
- 2) DR event 2 for the event during 10:17 to 10:26 (9 minutes),
- 3) DR event 3 for the event during 10:54 to 11:00 (6 minutes),
- 4) DR event 4 for the event during 12:15 to 14:15 (2 hours).

Due to the short-interval (< 10 minutes) variation of the power generation from the DGs, the first three DR events are activated using the 10-minute DR scheme by controlling ACs

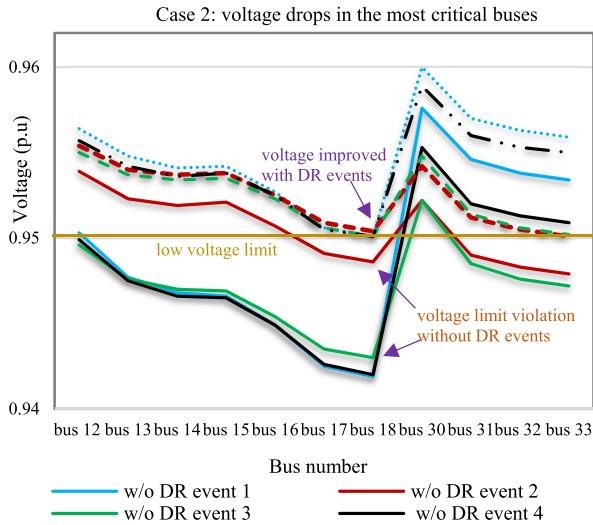


**FIGURE 9. Voltage profiles of critical buses with and without (w/o) DR deployment.**

and EHWs. The DR event 4 is activated using the 2-hour DR scheme due to the long-interval voltage variation in the network. Fig. 9 shows the bus voltages with and without the optimized DR events activation. It shows that the violated bus voltages are improved significantly with the proposed approach.

Fig. 10 shows the average voltage and power loss sensitivity values in respect to active power change in each bus in order to identify the DR candidate buses for the DR events. The DR candidate buses for each DR event are selected based on the highest combination of the sensitivity values, as explained in Section II.B.

Fig. 11 depicts the optimized incentive rates for the selected candidate buses in each DR event, and as seen, the incentive rate varies in each DR event and location. The optimized incentive rates increase as the total bus sensitivity values increase. As seen, the voltage improvement cost coefficient  $k_2$  is larger for all DR events than the loss improvement cost coefficient  $k_3$ , which is due to the voltage violation is being penalized more than other criteria.

Fig. 11 optimized incentive rates with  $k_i$  values for DR buses in all DR events. These  $k_i$  values are optimized in such way that the DR consumers located at the sensitive buses receive their fair incentive rated based on their contribution in the voltage and power loss improvement in the network. Table 3 presents the optimized results for all DR events in Case 2 with the proposed voltage control algorithm. It shows that the total DR (kW) used in each DR event varies and depends on the voltage violation magnitude and power loss minimization. It can be seen from Table 3 that the proposed load controller reduces the power loss in all DR events. In all the DR events in Case 2, the optimized switching of the DR appliances was enough to minimize the voltage violations in the network. Thus, not reactive power injection was required

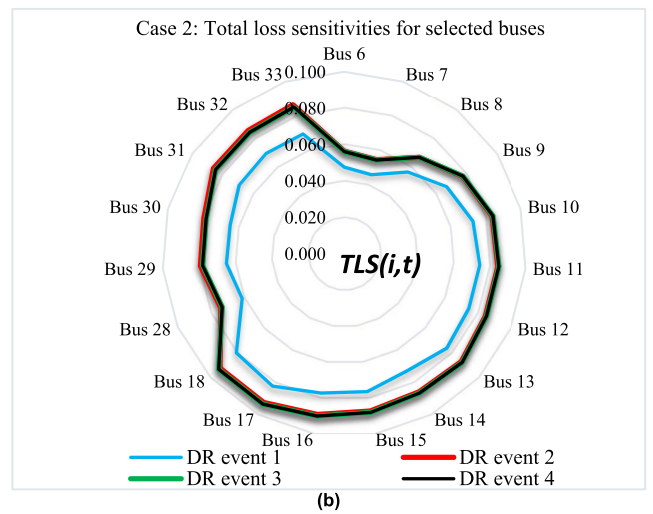
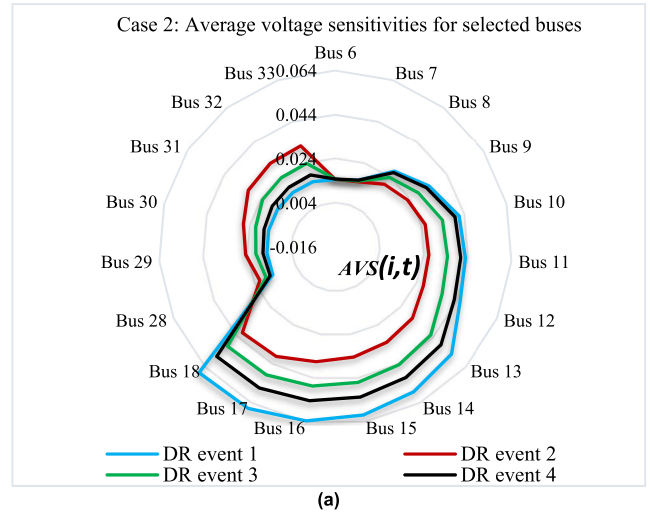


**FIGURE 10. (a) Average voltage sensitivities and (b) Total loss sensitivities for selected buses.**

**TABLE 3. Results of the proposed voltage management approach (VMA).**

| Case 2, no VMA |                   | After VMA implementation (optimized values) |         |                  |             |             |           |              |
|----------------|-------------------|---|---------|------------------|-------------|-------------|-----------|--------------|
| DR event#      | $P_{T,loss}$ (kW) | $P_{T,loss}$ (kW)                           | DR (kW) | $DR_{cost}$ (\$) | Penalty ADR | Penalty AFI | DGs' kVar | OF cost (\$) |
| 1              | 68.9              | 58.9  | 148.7   | 4.7              | 0           | 60          | 0         | 123.6        |
| 2              | 79.4              | 73.3  | 68.4    | 2.6              | 0           | 0           | 0         | 76.0         |
| 3              | 82.1              | 70.2  | 146.6   | 3.9              | 0           | 60          | 0         | 134.1        |
| 4              | 72.9              | 55.9  | 280.9   | 77.2             | 0           | 0           | 0         | 133.2        |

from the DGs. The owner of the DGs can maximize the use of the DGs' capacity to freely produce maximum amount of active power to the grid depending on the weather conditions. The AFI (appliance fair interruption) is violated for DR events 1 and 3 for some DR participants. It is due to those particular

DR participants are located in the sensitive buses in the network and required to control more appliances that other participants to satisfy the voltage limit constraints. Therefore, a small penalty factor (60) is added into the total objective

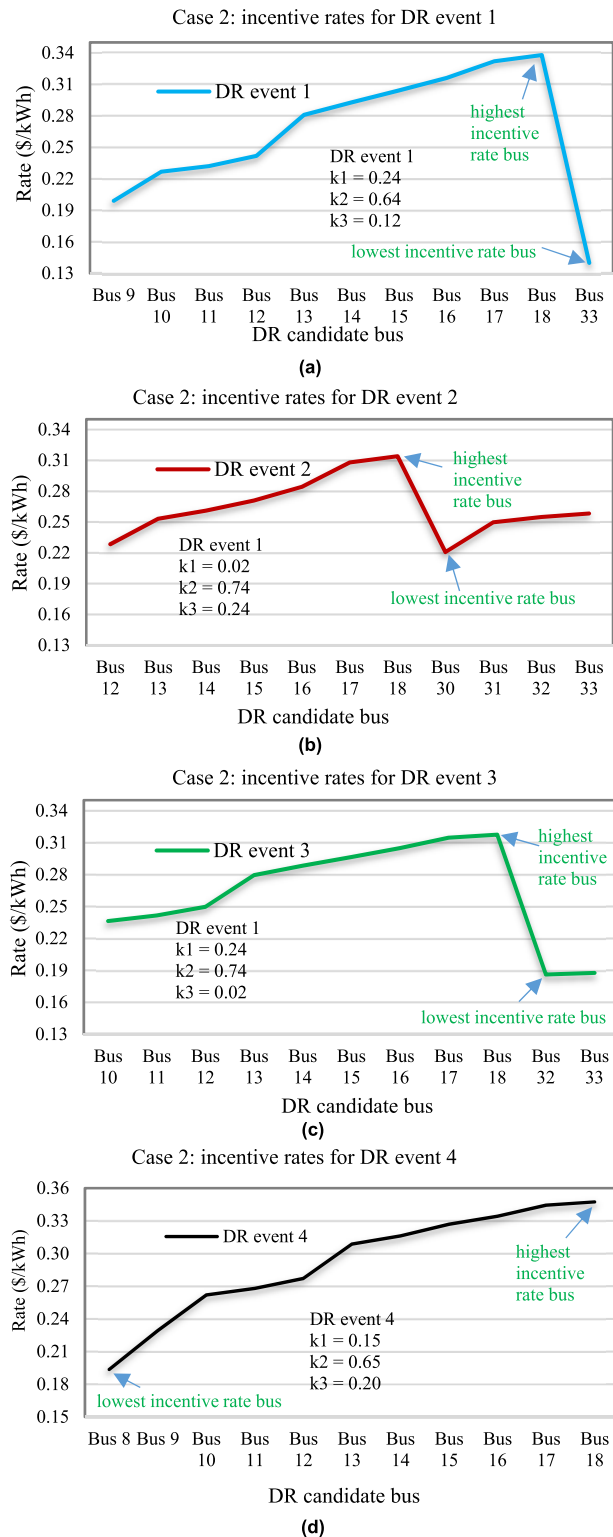


**FIGURE 11.** Optimized incentive rates with  $k_i$  values for DR buses in all DR events.

cost for 6 consumers in DR events 1 and 3. The proposed voltage management algorithm found the optimum solution by prioritizing the voltage violation reduction over the AFI violation.

**TABLE 4.** number of appliances controlled in case 1 and case 2.

|               | W.mc* |    | Dish* |    | Dryer |    | Pump |    | EV  |    | AC  |    | EWH |    |
|---------------|-------|----|-------|----|-------|----|------|----|-----|----|-----|----|-----|----|
|               | Off   | On | Off   | On | Off   | On | Off  | On | Off | On | Off | On | Off | On |
| Initial cond. | 41    | 49 | 57    | 33 | 66    | 24 | 54   | 36 | 30  | 60 |     |    |     |    |
| DR event 1    | 0     | 0  | 0     | 0  | 18    | 0  | 25   | 0  | 55  | 0  |     |    |     |    |
| DR event 2    | 0     | 0  | 0     | 0  | 35    | 0  | 13   | 0  | 29  | 0  |     |    |     |    |
| Initial cond. | 38    | 52 | 42    | 48 | 52    | 38 | 29   | 71 | 35  | 55 | 39  | 51 | 51  | 39 |
| DR event 1    |       |    |       |    |       |    |      |    |     |    | 28  | 0  | 35  | 0  |
| DR event 2    |       |    |       |    |       |    |      |    |     |    | 7   | 0  | 15  | 0  |
| DR event 3    |       |    |       |    |       |    |      |    |     |    | 28  | 0  | 34  | 0  |
| DR event 4    | 0     | 0  | 0     | 0  | 17    | 0  | 40   | 0  | 17  | 0  |     |    |     |    |

\*W.mc = washing machine; Dish=dishwasher

**C. APPLIANCES SWITCHING CONTROL FOR CASE 1 AND CASE 2**

Table 4 presents the number of appliances controlled during all DR events for a total 90 participated consumers in both Case 1 and Case 2. It shows the switching status (ON/OFF) of the participated appliances before and after each DR event. The DR events in Cases 1 and 2 reduce the consumers’ load demand to compensate for the active power drops from the DGs due to the clouding. The proposed algorithm determines the number of appliances to be switched off in each DR candidate bus to keep the voltage within the  $\pm 5\%$  limits and minimize the total power loss. The algorithm optimizes the switching of these appliances based on the constraints applied by the participated consumers on their consumption preferences and appliance switching (as explained in Section II.D). As shown in Table 4, in all the DR events of Case 1, the washing machine and dishwasher loads are not switched off when they are operating (ON condition), as their control preference is considered 3 (based on the definition in Table 1) during the optimization process they cannot be switched off while they are operating to avoid resetting the control cycles of these appliances. Since, the Case 1 has the long interval (1-2 hours) voltage problems as similar to DR event 4 in Case 2, the short usage of loads such as AC and EWH are not controlled in those DR events. Table 5 represents the randomly selected participated consumers’ appliances switching status before and during DR event 1 in both Case 1 and Case 2. It shows that consumer consumption preferences are prioritized in the proposed during voltage management in the network. Furthermore, the variability of kW demand (or rating) of each appliance and their participation availability in each DR event are considered in the optimization algorithm to provide a realistic DR implementation approach. A very few studies are available in the literature, which include this flexibility in the algorithm, as discussed in Section I.

**D. VALIDATION OF THE PROPOSED INCENTIVE METHOD**

In this section, the proposed dynamic DR incentive method for voltage control is compared with three different incentive methods. Fig. 12(a) shows different optimized incentive rates simulated for DR event 1 in Case 1, which are “Only power loss improvement rate”, “Only voltage

TABLE 5. Switching configurations for case 1 and case 2 in DR event 1.

| DR B# | Con# | Case 1                               |         |         |         |       |   |      |       |      |    | Case 2      |       |               |       |       |       |     |         |
|-------|------|--------------------------------------|---------|---------|---------|-------|---|------|-------|------|----|-------------|-------|---------------|-------|-------|-------|-----|---------|
|       |      | Initial condition (preference# / kW) |         |         |         |       | Optimized switching status $A_{n(i,t)}$ |      |       |      |    | Initial ... |       | Optimized ... |       |       |       |     |         |
|       |      | W.mc                                 | Dish    | Dryer   | Pump    | EV    | W.mc                                    | Dish | Dryer | Pump | EV | DR (\$)     | DR b# | Con#          | AC    | EHW   | AC    | EHW | DR (\$) |
| 8     | 2    | 0/0.6                                | 1/1.2   | 2/(n/a) | 1/2.0   | 1/3.0 | 0                                       | 1    | 0     | 0    | 1  | 0.317       | 9     | 1             | 3/1.1 | 0/4.5 | 1     | 0   | 0       |
|       | 4    | 0/1.8                                | 0/2.0   | 1/3.0   | 4/2.0   | 1/3.0 | 0                                       | 0    | 1     | 0    | 0  | 0.475       |       | 2             | 1/1.8 | 4/2.7 | 1     | 0   | 0       |
|       | 7    | 0/1.5                                | 2/(n/a) | 1/3.0   | 2/(n/a) | 1/3.0 | 0                                       | 0    | 1     | 0    | 0  | 0.475       |       | 6             | 0/0.6 | 1/2.7 | 0     | 0   | 0.063   |
|       | 10   | 4/0.5                                | 0/1.2   | 0/3.0   | 0/1.0   | 1/6.0 | 0                                       | 0    | 0     | 0    | 0  | 0.951       |       | 8             | 1/0.2 | 0/2.7 | 0     | 0   | 0.044   |
| 14    | 58   | 1/1.9                                | 0/2.0   | 4/3.0   | 0/1.0   | 1/3.0 | 1                                       | 0    | 0     | 0    | 0  | 0.868       | 10    | 29            | 0/0.2 | 1/2.7 | 1     | 0   | 0.082   |
| 16    | 68   | 1/1.9                                | 0/2.0   | 0/3.0   | 1/1.0   | 3/3.0 | 1                                       | 0    | 0     | 1    | 1  | 0           | 13    | 40            | 4/0.5 | 1/2.7 | 0     | 0   | 0.092   |
| 17    | 79   | 1/2                                  | 0/2.0   | 0/3.0   | 3/1.0   | 1/3.0 | 1                                       | 0    | 0     | 1    | 0  | 0.965       | 14    | 46            | 0/0.6 | 1/2.7 | 0     | 1   | 0       |
| 18    | 84   | 4/1.8                                | 0/2.0   | 0/3.0   | 1/2.0   | 3/3.0 | 0                                       | 0    | 0     | 0    | 1  | 0.647       | 18    | 76            | 0/0.6 | 1/2.7 | 0     | 0   | 0.106   |
|       | 85   | 2/(n/a)                              | 0/1.5   | 0/3.0   | 1/2.0   | 1/3.0 | 0                                       | 0    | 0     | 0    | 0  | 1.617       |       | 78            | 1/1.9 | 4/4.5 | 0     | 0   | 0.075   |
|       | 89   | 1/0.2                                | 1/2.0   | 0/3.0   | 4/1.0   | 1/3.0 | 1                                       | 1    | 0     | 0    | 0  | 0.97        |       | 33            | 90    | 0/0.5 | 1/2.7 | 1   | 0       |

DR B#: DR Bus; Con#: consumer number; preference#: refer to Table I; kW: appliance kW rating; W.mc = washing machine; Dish=dishwasher; DR(\$): DR cost (\$); n/a = not available;  : represents device is not available;  : represents device preference setting not to turn on;   represents device preference setting not to turn off.

improvement rate”, “Fixed rate” and “Proposed rate”. “Only power loss improvement rate” uses power loss sensitivity factor (2d) for DR rate calculation in (2a); “Only voltage improvement rate” uses voltage sensitivity factor (2b) for DR rate calculation in (2a); “Fixed rate” uses the TOU price rate in (2a); and the “Proposed rate” combines power loss and voltage sensitivities and TOU price rates for DR rate calculation in (2a). It can be seen in Fig. 12(a), the “Proposed rate” scheme distributes the incentive proportionately across DR participated buses based on their contributions in the voltage and power loss improvement in the network. The proposed incentive rate is higher at the far end of DR buses and lower in the closer buses to the substation. The optimized incentive rate falls between the power loss and voltage improvement rates but closer toward the voltage improvement rate of each DR bus, as the main objective of the paper is voltage control. Fig. 12(b) presents the obtained objective function parameters using four different optimized DR incentive rates. The proposed incentive method provides the lowest value in the objective function variables (i.e., DR cost (\$), DR size (kW), Power loss (kW), and Objective function cost (\$)) compared to other incentive methods.

Table 5 shows the optimized switching positions of DR participated appliances using the proposed method for two different intervals of DR events: “Long-interval” and “Short-interval” respectively for Case 1 and Case 2. As can be observed, if the participated consumers don’t have some DR appliances, these non-available DR appliances are numbered as “2” (highlighted in orange in Table 5) in the optimization process according to the appliance preference definitions in Table 1. Therefore, the optimized switching position for those appliances is zero (not operating) for any DR event. The appliance preference number “4” (highlighted in blue) represents that the particular appliance is restricted to participate in the current DR event, it is due to the fact that the appliance has already participated in the previous event or participant restricted to participate in a particular DR event. Therefore, the optimized switching position for those appliances is also zero. Finally, the appliance preference number “3” (highlighted in red) indicates that the appliance is under priority preference and its current status is ON and

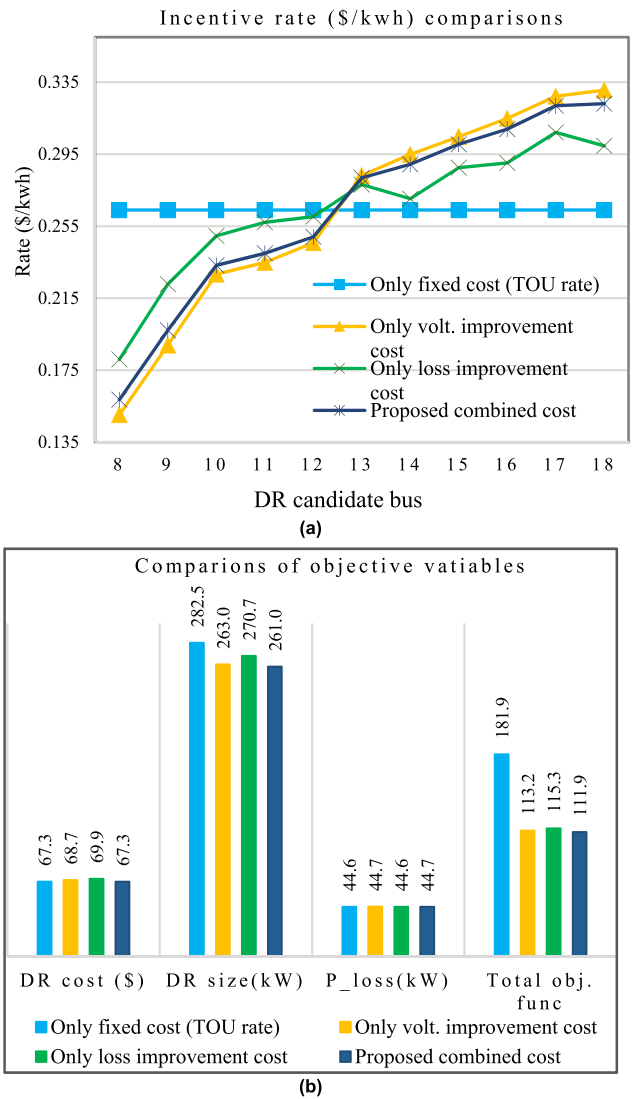


FIGURE 12. Comparisons of objective function variables using proposed and other incentive rate methods.

can’t be switched OFF in the DR event. It is due to the particular appliance can’t be interrupted while it is running (e.g., washing machine and dishwasher) to avoid hardware

damage or the appliance is prioritized to be ON for the owner's personal needs (e.g., the owner may need to charge the EV for traveling). Therefore, the optimized switching position for those appliances will not be changed (switching status is 1). The above-mentioned appliance's switching preferences are important for the optimization process in order to keep a record of the consumers' DR participant history and maintain their consumption preference and comfort levels in each DR event.

Table 5 shows the optimized switching positions of DR participated appliances using the proposed method for two different intervals of DR events: "Long-interval" and "Short-interval" respectively for Case 1 and Case 2. As can be observed, if the participated consumers don't have some DR appliances, these non-available DR appliances are numbered as "2" (highlighted in orange in Table 5) in the optimization process according to the appliance preference definitions in Table 1. Therefore, the optimized switching position for those appliances is zero (not operating) for any DR event. The appliance preference number "4" (highlighted in blue) represents that the particular appliance is restricted to participate in the current DR event, it is due to the fact that the appliance has already participated in the previous event or participant has been restricted to participate in a particular DR event. Therefore, the optimized switching position for those appliances is also zero. Finally, the appliance preference number "3" (highlighted in red) indicates that the appliance is under priority preference and its current status is ON and can't be switched OFF in the DR event. It is due to the particular appliance can't be interrupted while it is running (e.g., washing machine and dishwasher) to avoid hardware damage or the appliance is prioritized to be ON for the owner's personal needs (e.g., the owner may need to charge the EV for traveling). Therefore, the optimized switching position for those appliances will not be changed (switching status is 1). The above-mentioned appliance's switching preferences are important for the optimization process in order to keep a record of the consumers' DR participant history and maintain their consumption preference and comfort levels in each DR event.

### E. PERFORMANCE ANALYSIS OF THE PROPOSED IHPSO ALGORITHM

The objection function (OF) in (1a) is tested using different classic PSO algorithms and compared with the proposed IHPSO (improved hybrid particle swarm) algorithm. Using each PSO algorithm, the OF is run 10 times to get the best optimized result and standard deviation. Table 6 presents the comparison of the optimized results for DR event 1 in Case 1 using different PSO methods. It shows that with the MPSO (modified particle swarm) method, the optimization time is the lowest (32.32 sec.). However, it has a higher objective function and standard deviation as compared to the HPSO (hybrid particle swarm) and IHPSO methods. With the

**TABLE 6. Optimized results comparisons between different PSO methods.**

| Criteria                 | PSO    | MPSO   | HPSO  | IHPSO (proposed) |
|--------------------------|--------|--------|-------|------------------|
| Optimization time (sec.) | 37.33  | 32.32  | 51.02 | 50.13            |
| Best OF. result          | 10,569 | 10,493 | 112.4 | 111.9            |
| Standard deviation       | 2.2    | 1.9    | 1.5   | 0.70             |

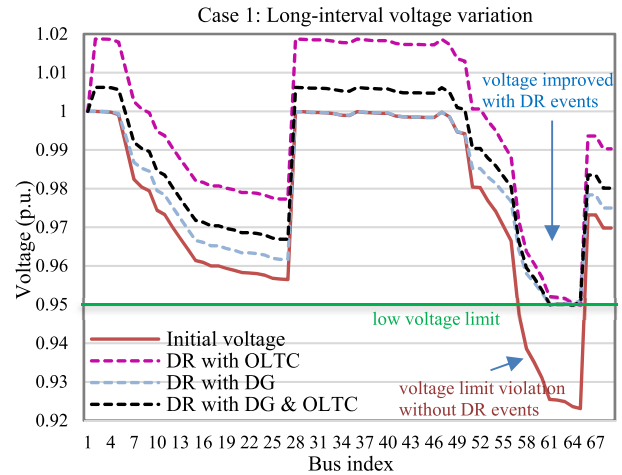


**FIGURE 13. Global best solution during searching process using different PSO methods.**

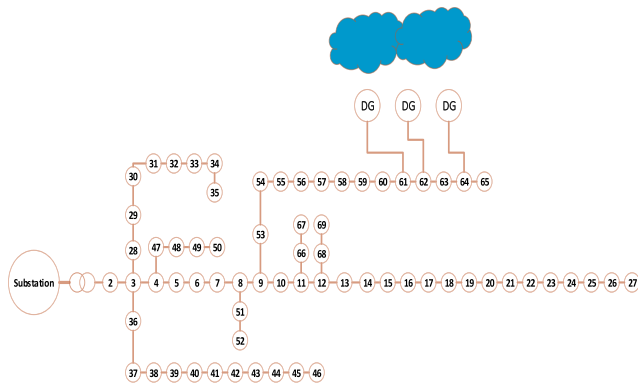
proposed IHPSO method the total objective function cost and the standard deviation are the lowest among all methods and with a slight increase in the optimization time compared to the PSO and MPSO methods. The optimization time in the PSO and MPSO is less because these methods don't have any hybridization approach with another optimization method, as a result, the OF result is very high as compared to the proposed IHPSO method. Therefore, the proposed IHPSO algorithm improves the OF performance and the accuracy of the voltage control algorithm.

Fig. 13 depicts the obtained global best solution curve during 100 iterations from all optimization methods. In all these PSO methods when Pbest and Gbest stopped updating for a period of time, it means a local optimal solution is found, as seen in Fig. 13. It can be observed that the classic PSO method stopped updating the optimization result after 50<sup>th</sup> iteration and MPSO method after 40<sup>th</sup> iteration. MPSO shows better performance than the classical PSO method due to a mutation function as equivalent to GA algorithm is added into MPSO. The proposed IHPSO method stopped updating at around 70<sup>th</sup> iteration with a global best value of 11.9, while HPSO stopped at 80<sup>th</sup> with the value of 112.4. The IHPSO outperforms the HPSO method by reducing the optimization time and objective function value. In IHPSO method, the GA mutation function and PS algorithm help the particle to jump out of the local optimum and enhance the chance of finding the global optimal solution.

**TABLE 7. Results of the proposed voltage management approach (VMA) in a large network (69 bus-system).**

| Solution approaches | After VMA implementation (optimized values) |            |         |             |               |                                     |                   |              |
|---------------------|---|------------|---------|-------------|---------------|-------------------------------------|-------------------|--------------|
|                     | Load (MVA)                                  | Ploss (kW) | DR (kW) | DRcost (\$) | OLTC tap (pu) | DG (kVAr)                           | OF (\$)           | Run time (s) |
| No VMA              | 4.655                                       | 181.9      | -       | -           | 1             | DG61,62,64 =0                       | -                 | -            |
| DR with OLTC        | 4.626                                       | 154.92     | 167     | 44.09       | 1.0188        | DG61,62,64 =0                       | 3366 <sup>a</sup> | 125.7        |
| DR with DG          | 3.958                                       | 96.33      | 159.5   | 42.11       | -             | DG61 =401<br>DG62 =401<br>DG64 =401 | 658.8             | 119.8        |
| DR with DG & OLTC   | 4.091                                       | 104.8      | 120.5   | 32.3        | 1.00625       | DG61 =248<br>DG62 =306<br>DG64 =356 | 1530 <sup>a</sup> | 109          |

<sup>a</sup>A high penalty cost ( $10^3$ ) is added in the optimization for each tap position changes in order to minimize the tap changing



**FIGURE 14. IEEE 69-bus MV network with multiple DG connections.**

**F. VALIDATION OF THE PROPOSED METHOD IN A LARGE NETWORK**

To validate the performance of the proposed voltage management method in a larger scale distribution network with many DR participated consumers and its coordination approach with the network element, an IEEE 69-bus system [46] is considered in the simulation. The optimum locations of the large solar PV-based DGs in the IEEE 69-bus network (in Fig. 14) are studied in [41]. The capacity of each DG is 1.22MW with a maximum power factor range  $\pm 0.95$  is considered. A total 14 DR candidate bus locations are identified out of 69 buses in the network according to the highest combined bus voltage sensitivity (2e) and the total loss sensitivity (2c) values of the buses, as explained in Section 2.B. The selected bus locations bus 24 to 27 and 56 to 65. A total 115 DR participants are considered randomly across the 14 DR candidate buses. Each participant is assumed to have a maximum 5 DR appliances for the long-interval voltage management (as described in Section 2.C). Therefore, the maximum DR participant appliances in the optimization process are 575 ( $115 \times 5$ ). It is assumed that during a high loading period in the network, a huge cloud movement causes the total active power production from DGs dropped to 10% (i.e. 366MW) from their total available capacity (i.e. 3660MW). As a result, the voltages at the far end buses drop significantly, as shown in Fig. 15. In this case, the long-interval DR scheme is initiated to solve the under-voltage problem using different

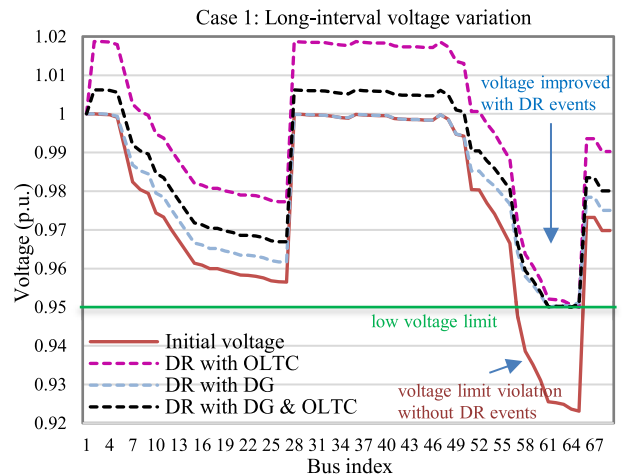


**FIGURE 15. Optimized voltage profiles of 69 buses with different DR coordination approaches.**

coordination approaches, which are DR with DGs’ reactive power, DR with OLTC (on-load tap changer located between bus 1 and 2) [46], and DR combined with DG and OLTC. As seen, from the optimized voltage profiles in Fig. 15, it can be seen that the DR with OLTC coordination approach provides slightly better voltage improvement at the far end buses as compared to other coordination approaches. However, it increases the voltage significantly at the buses closer to the substation. On the other hand, using the DR with DG and OLTC coordination approach provides a smooth variation of the bus voltages across the network compared to all other DR coordination approaches.

Table 7 shows the different optimized variables obtained from each DR coordinated voltage management approach. As explained above, the voltage management approach (VMA) using DR with DG and OLTC provides better voltage management across all buses in the network. However, the optimized objective function cost associated with this solution is quite high compared to DR with DG solution, as shown in Table 7. It is due to an additional cost in the objective function in (1a) is added for each tap change of the OLTC. The optimized cost using DR with DG approach is the lowest amongst the three voltage management approaches. Therefore, DR with DG approach can be a suitable and



frequently useable voltage management solution for all network conditions.

## V. CONCLUSION

This paper proposes a dynamic incentive based load control algorithm using household appliances through home energy management systems for managing both short- and long-interval voltage variations in the MV networks due to intermittent power output from solar DGs. Two DR schemes namely 10-minute and 2-hour DR schemes are proposed which can coordinate the network equipment such as reactive control from DGs and OLTC to compensate the short- and long-interval voltage variations, respectively. A dynamic location ranking method is proposed, which calculates the sensitivity values of voltage and total power loss to identify the most suitable DR candidate buses and distribute incentives fairly to DR participated consumers. Furthermore, each participating consumer's consumption preferences are prioritized in the DR event to maintain their comfort level. Finally, an improved version of the hybrid PSO algorithm (IHPSO) is proposed in the load controller, which is hybridization of the modified PSO (MPSO) and Pattern Search

(PS) algorithms to provide faster convergence and better optimisation results. The proposed load control method is first verified and tested using an IEEE 33-bus network considering high intermittent power generation from the DGs. The simulation results show that the load control algorithm successfully manages both short and long-interval voltage variations in the network. It minimises the excessive disturbances on consumers' loads, reduces the total cost of voltage compensation, prioritises the consumers' consumption preferences, and fairly incentivises the consumers based on their contributions. The proposed IHPSO heuristic optimisation technique provides better optimisation results and reduces the optimisation time. Finally, the proposed load control method is tested using a large network (IEEE 69-bus network) with many DR participated consumers to validate its performance in voltage control using different coordination approaches with the network voltage regulation devices such as OLTC. The performance of the proposed IHPSO algorithm will be further compared and tested with other optimisation algorithms such as the bi-level metaheuristic-based algorithm and interval analysis methods to validate its robustness.

## REFERENCES

- [1] J. Hu, X. Liu, M. Shahidehpour, and S. Xia, "Optimal operation of energy hubs with large-scale distributed energy resources for distribution network congestion management," *IEEE Trans. Sustain. Energy*, vol. 12, no. 3, pp. 1755–1765, Jul. 2021.
- [2] G. K. Ari and Y. Baghzouz, "Impact of high PV penetration on voltage regulation in electrical distribution systems," in *Proc. Int. Conf. Clean Electr. Power (ICCEP)*, Ischia, Italy, Jun. 2011, pp. 744–748.
- [3] R. Yan and T. K. Saha, "Investigation of voltage stability for residential customers due to high photovoltaic penetrations," *IEEE Trans. Power Syst.*, vol. 27, no. 2, pp. 651–662, May 2012.
- [4] B. Zhang, A. Y. S. Lam, A. Domínguez-García, and D. Tse, "An optimal and distributed method for voltage regulation in power distribution systems," *IEEE Trans. Power Syst.*, vol. 30, no. 4, pp. 1714–1726, Jun. 2015.
- [5] Y. Wang, T. Zhao, C. Ju, Y. Xu, and P. Wang, "Two-level distributed Volt/VAr control using aggregated PV inverters in distribution networks," *IEEE Trans. Power Del.*, vol. 35, no. 4, pp. 1844–1855, Aug. 2020.
- [6] Y. Wang, M. H. Syed, E. Guillo-Sansano, Y. Xu, and G. M. Burt, "Inverter-based voltage control of distribution networks: A three-level coordinated method and power hardware-in-the-loop validation," *IEEE Trans. Sustain. Energy*, vol. 11, no. 4, pp. 2380–2391, Oct. 2020.
- [7] L. Bhamidi and S. Sivasubramani, "Optimal planning and operational strategy of a residential microgrid with demand side management," *IEEE Syst. J.*, vol. 14, no. 2, pp. 2624–2632, Jun. 2020.
- [8] X. Liu, B. Gao, C. Wu, and Y. Tang, "Demand-side management with household plug-in electric vehicles: A Bayesian game-theoretic approach," *IEEE Syst. J.*, vol. 12, no. 3, pp. 2894–2904, Sep. 2018.
- [9] A. Khalid, N. Javaid, M. Guizani, M. Alhussein, K. Aurangzeb, and M. Ilahi, "Towards dynamic coordination among home appliances using multi-objective energy optimization for demand side management in smart buildings," *IEEE Access*, vol. 6, pp. 19509–19529, 2018.
- [10] X. Jiang and C. Xiao, "Household energy demand management strategy based on operating power by genetic algorithm," *IEEE Access*, vol. 7, pp. 96414–96423, 2019.
- [11] M. M. Rahman, A. Alfaki, G. M. Shafiullah, M. A. Shoeb, and T. Jamal, "Demand response opportunities in residential sector incorporated with smart load monitoring system," in *Proc. IEEE Innov. Smart Grid Technol.-Asia (ISGT-Asia)*, Melbourne, VI, Australia, Nov. 2016, pp. 1183–1188.
- [12] A. Zakariyadeh, O. Homaei, S. Jadid, and P. Siano, "A new approach for real time voltage control using demand response in an automated distribution system," *Appl. Energy*, vol. 117, pp. 157–166, Mar. 2014.
- [13] A. Arefi, A. Abeygunawardana, and G. Ledwich, "A new risk-managed planning of electric distribution network incorporating customer engagement and temporary solutions," *IEEE Trans. Sustain. Energy*, vol. 7, no. 4, pp. 1646–1661, Oct. 2016.
- [14] H. Chen, T. Ding, L. Chen, and J. Shi, "A modified harmonic pricing scheme for customers based on quantifying the harmonic comprehensive contribution," *Int. J. Electr. Power Energy Syst.*, vol. 130, Sep. 2021, Art. no. 106905.
- [15] J. Yang, F. Wu, J. Yan, Y. Lin, X. Zhan, L. Chen, S. Liao, J. Xu, and Y. Sun, "Charging demand analysis framework for electric vehicles considering the bounded rationality behavior of users," *Int. J. Electr. Power Energy Syst.*, vol. 119, Jul. 2020, Art. no. 105952.
- [16] K. Mahmud, A. K. Sahoo, and J. Ravishanker, "A day-ahead peak shaving strategy using aggregated electric vehicles," in *Proc. IEEE Energy Convers. Congr. Expo. (ECCE)*, Baltimore, MD, USA, Sep. 2019, pp. 6749–6753.
- [17] A. Ali, K. Mahmoud, and M. Lehtonen, "Optimal planning of inverter-based renewable energy sources towards autonomous microgrids accommodating electric vehicle charging stations," *IET Gener., Transmiss. Distrib.*, vol. 16, no. 2, pp. 219–232, Jan. 2022.
- [18] A. Ali, K. Mahmoud, and M. Lehtonen, "Optimization of photovoltaic and wind generation systems for autonomous microgrids with PEV-parking lots," *IEEE Syst. J.*, vol. 16, no. 2, pp. 3260–3271, Jun. 2022.
- [19] A. Ali, D. Raisz, and K. Mahmoud, "Optimal scheduling of electric vehicles considering uncertain RES generation using interval optimization," *Electr. Eng.*, vol. 100, no. 3, pp. 1675–1687, Sep. 2018.
- [20] M. Muratori and G. Rizzoni, "Residential demand response: Dynamic energy management and time-varying electricity pricing," *IEEE Trans. Power Syst.*, vol. 31, no. 2, pp. 1108–1117, Mar. 2016.
- [21] J. Wang, Y. Shi, and Y. Zhou, "Intelligent demand response for industrial energy management considering thermostatically controlled loads and EVs," *IEEE Trans. Ind. Informat.*, vol. 15, no. 6, pp. 3432–3442, Jun. 2019.
- [22] S. M. Ghorashi, M. Rastegar, S. Senemmar, and A. R. Seifi, "Optimal design of reward-penalty demand response programs in smart power grids," *Sustain. Cities Soc.*, vol. 60, Sep. 2020, Art. no. 102150.
- [23] Q. Xie, H. Hui, Y. Ding, C. Ye, Z. Lin, P. Wang, Y. Song, L. Ji, and R. Chen, "Use of demand response for voltage regulation in power distribution systems with flexible resources," *IET Gener., Transmiss. Distrib.*, vol. 14, no. 5, pp. 883–892, Mar. 2020.
- [24] C. Roy and D. K. Das, "A hybrid genetic algorithm (GA)-particle swarm optimization (PSO) algorithm for demand side management in smart grid considering wind power for cost optimization," *Sādhanā*, vol. 46, no. 2, pp. 1–12, Jun. 2021.
- [25] T. A. Nakabi and P. Toivanen, "Deep reinforcement learning for energy management in a microgrid with flexible demand," *Sustain. Energy, Grids Netw.*, vol. 25, Mar. 2021, Art. no. 100413.

- [26] X. Zhu, J. Yang, Y. Liu, C. Liu, B. Miao, and L. Chen, "Optimal scheduling method for a regional integrated energy system considering joint virtual energy storage," *IEEE Access*, vol. 7, pp. 138260–138272, 2019.
- [27] S. Shao, M. Pipattanasomporn, and S. Rahman, "An approach for demand response to alleviate power system stress conditions," in *Proc. IEEE Power Energy Soc. Gen. Meeting*, Detroit, MI, USA, Jul. 2011, pp. 1–7.
- [28] F. A. Wolak. (Feb. 2007). *Residential Customer Response to Real-Time Pricing: The Anaheim Critical Peak Pricing Experiment*. UC Berkeley. Accessed: Feb. 2021. [Online]. Available: <https://escholarship.org/uc/item/3td3n1x1>
- [29] *Synergy Smart Home Plan*. Accessed: May 2021. [Online]. Available: <https://www.synergy.net.au/Your-home/Energy-plans/Smart-Home-Plan>
- [30] M. A. Tolba, V. N. Tulsy, and A. A. Z. Diab, "Optimal allocation and sizing of multiple distributed generators in distribution networks using a novel hybrid particle swarm optimization algorithm," in *Proc. IEEE Conf. Russian Young Researchers Electr. Electron. Eng. (EIConRus)*, St. Petersburg, Russia, Feb. 2017, pp. 1606–1612.
- [31] D. S. Watson, "Fast automated demand response to enable the integration of renewable resources," Lawrence Berkeley Nat. Lab., Berkeley, CA, USA, Tech. Rep. CEC-XXX-2012-XXX, Apr. 2013.
- [32] M. Pipattanasomporn, M. Kuzlu, S. Rahman, and Y. Teklu, "Load profiles of selected major household appliances and their demand response opportunities," *IEEE Trans. Smart Grids*, vol. 5, no. 2, pp. 742–750, Mar. 2014.
- [33] Steadysun Thenergy White Paper. (Apr. 2016). *Energy Generation Forecasting in Solar-Diesel-Hybrid Applications*. Accessed: May 2021. [Online]. Available: [http://steady-sun.com/wp-content/uploads/2016APR-Study\\_SkyImager\\_for\\_Hybrid.pdf](http://steady-sun.com/wp-content/uploads/2016APR-Study_SkyImager_for_Hybrid.pdf)
- [34] T. Logenthiran, D. Srinivasan, and T. Z. Shun, "Demand side management in smart grid using heuristic optimization," *IEEE Trans. Smart Grid*, vol. 3, no. 3, pp. 1244–1252, Sep. 2012.
- [35] T. P. I. Ahamed, S. D. Maqbool, and N. Malik, "A reinforcement learning approach to demand response," in *Proc. Centenary Conf. EE II-Sc*, Bangalore, India, 2011.
- [36] S. Q. Ali, I. A. T. Parambath, and N. H. Malik, "Learning automata algorithms for load scheduling," *Electr. Power Compon. Syst.*, vol. 41, no. 3, pp. 286–303, Feb. 2013.
- [37] M. Clerc and J. Kennedy, "The particle swarm—Explosion, stability, and convergence in a multidimensional complex space," *IEEE Trans. Evol. Comput.*, vol. 6, no. 1, pp. 58–73, Feb. 2002.
- [38] A. Azizivahed, A. Arefi, S. Ghavidel, M. Shafie-Khan, L. Li, J. Zhang, and J. P. S. Catalao, "Energy management strategy in dynamic distribution network reconfiguration considering renewable energy resources and storage," *IEEE Trans. Sustain. Energy*, vol. 11, no. 2, pp. 662–673, Apr. 2020.
- [39] Y. Labbi and D. B. Attous, "A hybrid particle swarm optimization and pattern search method to solve the economic load dispatch problem," *Int. J. Syst. Assurance Eng. Manage.*, vol. 5, no. 3, pp. 435–443, Sep. 2014.
- [40] J.-H. Teng, "A direct approach for distribution system load flow solutions," *IEEE Trans. Power Del.*, vol. 18, no. 3, pp. 882–887, Jul. 2003.
- [41] M. M. Aman, G. B. Jasmon, A. H. A. Bakar, and H. Mokhlis, "A new approach for optimum simultaneous multi-DG distributed generation Units placement and sizing based on maximization of system loadability using HPSO (hybrid particle swarm optimization) algorithm," *Energy*, vol. 66, no. 4, pp. 202–215, 2014.
- [42] S. Sayeef, S. Heslop, D. Cornforth, T. Moore, S. Percy, J. Ward, A. Berry, and D. Rowe, "Solar intermittency: Australia's clean energy challenge. Characterising the effect of high penetration solar intermittency on Australian electricity networks," CSIRO, Newcastle, NSW, Australia, Tech. Rep. EP121914, Jun. 2012.
- [43] M. M. Rahman, "Modelling and analysis of demand response implementation in the residential sector," Ph.D. thesis, Elect. Eng., Murdoch Univ., Perth, WA, Australia, 2018.
- [44] X. Li and S. Wang, "A review on energy management, operation control and application methods for grid battery energy storage systems," *CSEE J. Power Energy Syst.*, vol. 7, no. 5, pp. 1–15, 2019.
- [45] J. Yang, W. Sun, G. Harrison, and J. Robertson, "A novel planning method for multi-scale integrated energy system," in *Proc. IEEE Milan PowerTech*, Milan, Italy, Jun. 2019, pp. 1–6.
- [46] J. S. Savier and D. Das, "Impact of network reconfiguration on loss allocation of radial distribution systems," *IEEE Trans. Power Del.*, vol. 22, no. 4, pp. 2473–2480, Oct. 2007.



**MD MOKTADIR RAHMAN** received the B.S. degree in electrical engineering from the American University of Bangladesh, in 2008, the M.Sc. and M.Phil. degrees in power system and renewable energy from City University London, U.K., in 2011 and 2015, respectively, and the Ph.D. degree in electrical engineering from Murdoch University, Australia, in 2018.

He worked as a Power System Engineer at OST Energy, U.K., after completing his M.Sc. degree.

He is currently working as a Senior Power System Engineer at Essential Energy, Australia. He has more than eight years of experience in the power and renewable energy engineering sectors. He was involved grid connection and modeling of more than 3GW of Solar PV and battery projects implementation across Australia. He is a Partner Investigator in the "ARC Training Centre in Energy Technologies for Future Grids" Project, which is in one of the largest ARC-funded (5 Million AUD) projects in the energy sector of Australia. He received several competitive awards throughout his academic and industry careers. He was awarded two postdoctoral positions in Australia funded by ARENA and the City of Melville in Western Australia, after completion of his Ph.D. degree. His research interests include the large-scale renewable generator integrations, grid forming converters, power system stability, and demand side management in the distribution networks.



**ALI AREFI** (Senior Member, IEEE) received the B.Sc., M.Sc., and Ph.D. degrees in electrical engineering, in 1999, 2001, and 2011, respectively. He has six years experience with electric distribution industry in the fields of planning, loss reduction, power quality, and distributed generation integration within electric distribution networks. He has conducted power quality and energy audits for several industries and electric distribution companies. He was a Lecturer and a Research

Fellow with the Queensland University of Technology, until 2015. He is currently an Associate Professor with the Discipline of Engineering and Energy, Murdoch University, Perth, Australia. His research interests include the areas of electric delivery planning, state estimation, power quality, and energy efficiency.



**G. M. SHAFIULLAH** received the bachelor's degree in engineering from the Chittagong University of Engineering Technology, Bangladesh, and the master's and Ph.D. degrees from Central Queensland University, Australia, in 2009 and 2013, respectively. He is currently an Associate Professor at Murdoch University, Perth, Australia. He has authored 120 book chapters, journal articles, and conference papers in the areas of power systems, smart grid, and renewable energy.



**SUJEEWA HETTIWATTE** received the Ph.D. degree in electrical engineering and electronics from The University of Manchester (formerly UMIST), U.K. He is currently an Assistant Professor with the Department of Electrical and Electronic Engineering, Faculty of Engineering, Sri Lanka Institute of Information Technology, Malabe, Sri Lanka. He is also an Adjunct Lecturer at Murdoch University, Perth, Australia. He has research and teaching experience from Australia, New Zealand, and Sri Lanka.



**ALI AZIZVAHED** received the B.Sc. degree from the Razi University of Kermanshah, Kermanshah, Iran, in 2010, and the M.Sc. degree from the Shiraz University of Technology, Shiraz, Iran, in 2012, all in power electrical engineering. He is currently pursuing the Ph.D. degree in electrical engineering with the University of Technology Sydney, Sydney, Australia. Since April 2018, he has been collaborating with the School of Electrical and Electronic Engineering, Murdoch University, Perth, Australia. His research interests include large scale integration of renewable energy sources in smart grids, power systems reliability and stability, dynamic market and operation, and probabilistic programming.



**S. M. MUYEEN** (Senior Member, IEEE) received the B.Sc. (Eng.) degree in electrical and electronic engineering from the Rajshahi University of Engineering and Technology (RUET, formerly known as the Rajshahi Institute of Technology), Bangladesh, in 2000, and the M.Eng. and Ph.D. degrees in electrical and electronic engineering from the Kitami Institute of Technology, Japan, in 2005 and 2008, respectively. He is currently working as a Full Professor with the Electrical

Engineering Department, Qatar University. He has been a keynote speaker and an invited speaker at many international conferences, workshops, and universities. He has published more than 250 articles in different journals and international conferences. He has published seven books as the author or an editor. His research interests include power system stability and control, electrical machine, FACTS, energy storage systems (ESSs), renewable energy, and HVDC systems. He is a fellow of Engineers Australia. He is serving as an Editor/an Associate Editor for many prestigious journals from IEEE, IET, and other publishers, including *IEEE TRANSACTIONS ON ENERGY CONVERSION*, *IEEE POWER ENGINEERING LETTERS*, *IET Renewable Power Generation*, and *IET Generation, Transmission and Distribution*.



**MD. RABIUL ISLAM** (Senior Member, IEEE) received the Ph.D. degree in electrical engineering from the University of Technology Sydney (UTS), Sydney, Australia, in 2014. He is currently a Senior Lecturer with the School of Electrical, Computer, and Telecommunications Engineering (SECTE), University of Wollongong (UOW), New South Wales, Australia. He has authored or coauthored more than 320 papers, including 90 IEEE TRANSACTIONS/IEEE journal papers.

He has written or edited seven technical books published by Springer and Taylor & Francis. His research interests include the fields of power electronic converters, renewable energy technologies, power quality, electrical machines, electric vehicles, and smart grid. He has received several Best Paper Awards, including Two Best Paper recognitions from *IEEE TRANSACTIONS ON ENERGY CONVERSION*, in 2020. He is serving as an Associate Editor for the *IEEE TRANSACTIONS ON INDUSTRIAL ELECTRONICS*, *IEEE TRANSACTIONS ON ENERGY CONVERSION*, *IEEE POWER ENGINEERING LETTERS*, and *IEEE ACCESS*. As a Lead Guest Editor, he has organized the first joint IEEE Industrial Electronics Society and IEEE Power & Energy Society Special Section titled *Advances in High-frequency Isolated Power Converters*. He is an Editor of the Book Series titled *Advanced in Power Electronic Converters* (CRC Press, Taylor & Francis Group). He has received several funding from Government and Industries, including in total \$5.48 million from Australian Government through Australian Research Council (ARC) Discovery Project (DP) 2020 titled “A Next Generation Smart Solid-State Transformer for Power Grid Applications” and ARC Industrial Transformation Training Centre Project 2021 titled “ARC Training Centre in Energy Technologies for Future Grids.”

• • •